

Elsevier Editorial System(tm) for Virology
Manuscript Draft

Manuscript Number: VIRO-17-767R1

Title: Differential Phosphorylation and N-terminal Configuration of Capsid Subunits in Parvovirus Assembly and Viral Trafficking

Article Type: Regular Article

Section/Category: 2 Virus Structure and Assembly

Keywords: Parvovirus/capsid phosphorylation/Nt configuration/assembly/maturation/viral trafficking

Corresponding Author: Professor Jose M Almendral del Rio, PhD

Corresponding Author's Institution: Centro de Biologia Molecular Severo Ochoa (CSIC-UAM)

First Author: Jose M Almendral del Rio, PhD

Order of Authors: Jose M Almendral del Rio, PhD; Jon Gil-Ranedo, PhD; Eva Hernando-Monge, PhD; Noelia Valle, PhD; Laura Riolobos, PhD; Beatriz Maroto, PhD

Abstract: The T1 parvovirus Minute Virus of Mice (MVM) was used to study the roles that phosphorylation and N-terminal domains (Nt) configuration of capsid subunits may play in icosahedral nuclear viruses assembly. In synchronous MVM infection, capsid subunits newly assembled as two types of cytoplasmic trimeric intermediates (3VP2, and 1VP1:2VP2) harbored a VP1 phosphorylation level fivefold higher than that of VP2, and hidden Nt. Upon nuclear translocation at S phase, VP1-Nt became exposed in the heterotrimer and subsequent subviral assembly intermediates. Empty capsid subunits showed a phosphorylation level restored to VP1:VP2 stoichiometry, and the Nt concealed in their interior. However ssDNA-filled virus maturing at S/G2 lacked VP1 phosphorylation and one major VP2 phosphopeptide, and exposed VP2-Nt. Endosomal VP2-Nt cleavage resulted in VP3 subunits devoid of any phospholabel, implying that incoming viral particles specifically harbor a low phosphorylation status. Phosphorylation provides a mechanistic coupling of parvovirus nuclear assembly to the cell cycle.

VIROLOGY
Elsevier

February 15th, 2018

Dear Mr(s),

Enclosed please find the **revised version** of the manuscript entitled:

Differential Phosphorylation and N-terminal Configuration of Capsid
Subunits in Parvovirus Assembly and Viral Trafficking

contributed by Jon Gil-Ranedo, Eva Hernando, Noelia Valle, Laura Riobos, Beatriz Maroto,
and J.M. Almendral,

that we are re-submitting for consideration of publication in **VIROLOGY**.

Following the indications from the Editor, we are submitting a new version of the article addressing the questions raised by Reviewers'. For this, we have accordingly corrected some references, better explained the legend of Figure 7, and carefully revised the manuscript for words use and misspellings.

Enclosed please find the following documents and Figures:

1. The revised version of the Full-Text of the manuscript.
2. Seven Figures checked for quality.
3. Point-by-point responses to each of the issues raised by the reviewers.

We hope this revised version of the article be appropriate for publication in *Virology*.

Thank you very much for your time and consideration.

Looking forward to hearing from you.

Yours Sincerely,

José M. Almendral, PhD

Professor of Microbiology. Molecular Virology.
Centro de Biología Molecular "Severo Ochoa" (CSIC-UAM)
Universidad Autónoma de Madrid (UAM). Cantoblanco, 28049 Madrid. Spain.
E-mail: jmalmendral@cbm.csic.es. Phone: 34-91-1964559

VIRO-S-17-01066

Response to Reviewers

Reviewer #1:

The title reflects the nature of the study.

The introduction elegantly describes the essential background of the study.

The M&M is clear and in sufficient detail (reminds of approaches by Lombardo).

Figures are excellent and support results

Response: Thank you for these positive comments.

Results:

Small corrections:

– *p. 14 komma missing in line 26-27*

– *immunoprecipitation in native conditions of the 35S-labeled samples showed a 1:5 ratio of VP1:VP2 subunits in the assemblies, their approximate stoichiometry of synthesis, when using anti-VPs antibody, but a ratio close to 1:2 when anti VP1 antibody was used heterotrimer in G1/S arrested cells; thus, VP1 subunits assemble into a cytoplasmic 1VP1:2VP2.*

– *Phosphorylated proteins at a VP1:VP2 ratio close to 1.0. Therefore, on average, VP1 subunits assembled in cytoplasmic trimers harbored a phosphorylation level close to 5-fold higher than that of the VP2 subunits. Valid conclusions.*

– *Using derived genomic constructs lacking either VP1 or VP2 in transfections support results*

– *p.19 line 47: take out cleavage*

– *Change:*

Parrish, C.P. 2010. Structures and functions of parvovirus capsids and the process of cell infection. Curr. Top. Microbiol. Immunol. 343: 149-76.

to:

Parrish, C.R. 2010. Structures and functions of parvovirus capsids and the process of cell infection. Curr. Top. Microbiol. Immunol. 343: 149-176.

– *Change:*

Zadori, Z., Szelei, J., Lacoste, M.C., Gariépy, S., Raymond, P., Allaire, M., Nabi, I.R., and P. Tijssen. 2001. A viral phospholipase A2 is required for parvovirus infectivity. Dev. Cell 2: 291-302.

to:

Zadori, Z., Szelei, J., Lacoste, M.C., Gariépy, S., Raymond, P., Allaire, M., Nabi, I.R., and P. Tijssen. 2001. A viral phospholipase A2 is required for parvovirus infectivity. Dev. Cell 1: 291-302. Zhang, K., Brownlie, R., Snider, M., and S. van Drunen Littel-van den Hurka. 2016. should be: Zhang, K., Brownlie, R., Snider, M., and S. van Drunen Littel-van den Hurk. 2016.

Response: all these changes have been introduced in the revised version of the manuscript.

– *Fig. 7 could be clearer; what is the meaning here of G1->S->G2*

Response: this figure is intended to summarize our findings on the connection of virus assembly cycle with the steps of the host cell cycle. More specifically, the

level of VPs phosphorylation and N-terminal sequences exposure described in the preceding Figures 1 to 6 have been illustrated here connected with the cell cycle: nuclear transport of newly synthesized VPs occurs as trimers at early S phase, but viral genome packaging only take place at late S-G2. Anyhow, trying to satisfy the concern of the reviewer, we have added a sentence in the legend of this Figure 7 to clarify the purpose of the figure.

Reviewer #2:

The manuscript by Gil-Ranedo et al. extends and completes an extensive study by these authors of the synthesis, processing and assembly of the capsid subunits of the minute virus of mice (MVM). Their goal is to understand the roles of protein conformational changes and protein phosphorylation in relation to the cell cycle, which has an important impact on MVM infection.

The authors are very experienced in the methods they use and they describe them thoroughly. They employ cells engineered to express MVM capsid proteins as well as natural viral infections. The findings are clearly presented and support in general the conclusions. The authors showed previously that MVM capsid subunits assemble as homo- and hetero-trimeric intermediates in the cytoplasm and in the present work assume these and assembled capsids are the structures they observe by immunostaining.

Response: thank you for these positive comments on our work.

These observations are an important contribution to our understanding of the multifaceted control of particle assembly and maturation for this type of virus. The results lead to a model in which MVM cell entry and the subsequent synthesis, transport and assembly of new subunits is accompanied by changes in the exposure of VP1 and VP2 N-termini and in their phosphorylation levels. This model is complex and so the diagram in Figure 7 is helpful.

Response: thank you for the emphasis on the usefulness of this diagram.

Exactly why these changes are needed for the different steps of viral infection is unclear and will require further work.

Response: We certainly agree on that the elucidation of the precise function(s) of these VPs changes in the different steps of the viral infection cycle will require further work.

The text has some grammatical errors and occasional poor word choice, and could benefit from revision from this point of view.

Response: The text has been further checked for grammatical errors and word choice. We trust these aspects have been improved in the revised version of the manuscript.

This manuscript provides new insights into the role that capsid proteins phosphorylation and configuration play in viral assembly and traffic. Using the icosahedral (T1) nuclear parvovirus Minute Virus of Mice (MVM) as a model, we show changes of N-terminal sequences configuration and differential phosphorylation of capsid subunits, along the cell-cycle coupled nuclear translocation of viral assembly intermediates. Furthermore, a subsequent drastic though specific dephosphorylation of some capsid subunits is demonstrated as the viral genome becomes packaged. These findings highlight the complex regulations of life cycle steps even for small nuclear viruses, and increase our understanding of crucial virus-cell cycle interactions.

1
2
3
4
5 **Differential Phosphorylation and N-terminal**
6 **Configuration of Capsid Subunits in Parvovirus**
7 **Assembly and Viral Trafficking**
8
9

10
11
12
13
14
15 Jon Gil-Ranedo¹, Eva Hernando², Noelia Valle³, Laura Riolobos⁴, Beatriz Maroto⁵,

16
17
18 and José M. Almendral[#]
19
20

21 *Centro de Biología Molecular "Severo Ochoa" (Consejo Superior de Investigaciones*
22 *Científicas-Universidad Autónoma de Madrid), Cantoblanco, 28049 Madrid, Spain.*
23
24
25

26
27 **Running Title:** Structural proteins phosphorylation in parvovirus assembly and traffic
28
29
30
31

32 *Present address:* ¹Peninsula School of Medicine, Plymouth University, PL6 8BU
33 Plymouth, UK; ²Department of Pathology, NYU Cancer Center, NY10016, USA;
34 ³Departamento de Biotecnología, Universidad Francisco de Vitoria, Madrid, Spain;
35 ⁴Cancer Vaccine Institute, Center for Translational Medicine in Women's Health,
36 University of Washington, Seattle, WA 98109, USA.; ⁵NIMGenetics, PCM, 28049
37 Cantoblanco, Madrid, Spain.
38
39
40
41
42
43
44
45
46

47 [#]Corresponding author. Mailing address: José M. Almendral. Centro de Biología
48 Molecular "Severo Ochoa" (CSIC-UAM). Universidad Autónoma de Madrid.
49 Cantoblanco, 28049 Madrid. Spain. Phone: 34-91-1964559. Electronic mail address:
50 jmalmendral@cbm.csic.es.
51
52
53
54
55
56
57
58
59
60
61
62
63
64
65

Abstract

The T1 parvovirus Minute Virus of Mice (MVM) was used to study the roles that phosphorylation and N-terminal domains (Nt) configuration of capsid subunits may play in icosahedral nuclear viruses assembly. In synchronous MVM infection, capsid subunits newly assembled as two types of cytoplasmic trimeric intermediates (3VP2, and 1VP1:2VP2) harbored a VP1 phosphorylation level fivefold higher than that of VP2, and hidden Nt. Upon nuclear translocation at S phase, VP1-Nt became exposed in the heterotrimer and subsequent subviral assembly intermediates. Empty capsid subunits showed a phosphorylation level restored to VP1:VP2 stoichiometry, and the Nt concealed in their interior. However ssDNA-filled virus maturing at S/G2 lacked VP1 phosphorylation and one major VP2 phosphopeptide, and exposed VP2-Nt. Endosomal VP2-Nt cleavage resulted in VP3 subunits devoid of any phospholabel, implying that incoming viral particles specifically harbor a low phosphorylation status. Phosphorylation provides a mechanistic coupling of parvovirus nuclear assembly to the cell cycle.

Keywords: Parvovirus/capsid phosphorylation/Nt configuration/assembly/maturation/viral trafficking

Introduction

In eukaryotes, the activity of protein kinases contributes to many fundamental processes such as signal transduction, metabolism, and the cell cycle, by catalyzing the transfer of negatively charged phosphoryl moieties predominantly to serine, threonine, and tyrosine amino acid residues (Manning *et al.*, 2002; Ubersax and Ferrell, 2007). Viral proteins may serve as substrates for cellular or virus-encoded protein kinases, their phosphorylation influencing structure and function through conformational changes or direct chemical effects on protein interactions. Understanding the biological effect of phosphate substituents incorporated in virus structural proteins is challenged by their transient nature, technical difficulty to precisely map phosphorylation sites, and the lack of resolution in the 3-D structure of virus particles. Nevertheless phosphorylation of structural proteins of RNA and DNA viruses mediates processes key to their life cycles, such as recognition of cellular factors, assembly of viral components, genome packaging, or viral trafficking (e.g. Sugai *et al.*, 2014; Mondal *et al.*, 2015; Bjorn-Patrick and Roy, 2016; Zhang *et al.*, 2016), and may provide targets for antiviral therapies. Icosahedral DNA animal viruses (such as *Herpesviridae*, *Adenoviridae*, *Papillomaviridae*, *Polyomaviridae*, or *Parvoviridae*) whose structural components must traffick through the nuclear envelope to assemble and mature, conform a framework of viral systems to explore the diversity of functions played by capsid proteins phosphorylation.

With the aim of constructing a comprehensive virus model on this issue, we chose the *Protoparvovirus* Minute Virus of Mice (MVM), a reference member of the *Parvoviridae* (Cotmore *et al.*, 2014), and an important mouse pathogen (Brownstein *et al.*, 1991;

1
2
3
4 Ramirez *et al.*, 1996; Segovia *et al.*, 1999). Parvoviruses are nonenveloped eukaryotic
5
6 nuclear viruses containing a 5kb single-stranded (ss) DNA genome in a 25 nm-diameter
7
8 icosahedral (T=1) capsid made from two to three polypeptides. The MVM capsid is
9
10 composed of about ten subunits of the VP1 (83 kDa) and fifty subunits of the VP2 (64
11
12 kDa) proteins (Cotmore and Tattersall, 2014). The 3-D atomic structure of the capsid
13
14 resolved for many parvoviruses exhibits a common folding of the protein subunits in an
15
16 eight-stranded antiparallel β -barrel topology, whereas the capsid surface may differ
17
18 drastically due to prominent loops and depressions which confer characteristic functions
19
20 (Tsao *et al.*, 1991; Agbandje-McKenna *et al.*, 1998; Xie *et al.*, 2002; Kaufmann *et al.*,
21
22 2004; Kontou *et al.*, 2005; Gurda *et al.*, 2010). The N-terminal (Nt) sequences of the
23
24 parvovirus capsid proteins (VPs) are flexible sequences with generally unresolved structure
25
26 in the crystals, with the exception of Nt of the human B19 major capsid protein (Kaufmann
27
28 *et al.*, 2008). However these unordered Nt can be alternatively exposed on the surface of
29
30 the capsid in controlled processes to serve as trafficking signals at different stages of the
31
32 viral life cycle (Maroto *et al.*, 2004; Valle *et al.*, 2006). The unique VP1 Nt sequence (1Nt)
33
34 contains diverse protein motifs required by the incoming virus to initiate infection, such as
35
36 phospholipase A2 (PLA₂) activity (Zadori *et al.*, 2001; Farr *et al.*, 2005), nuclear
37
38 localization sequences (NLS) (Vihinen-Ranta *et al.*, 2002; Lombardo *et al.*, 2002;
39
40 Sonntang *et al.*, 2006; Johnson *et al.*, 2010; Boisvert *et al.*, 2014), and other functionally
41
42 uncharacterized domains (Tullis *et al.*, 1993; Lombardo *et al.*, 2002; Popa-Wagner *et al.*,
43
44 2012; Porwal *et al.*, 2013). The VP2 Nt sequence (2Nt) localized in the interior of empty
45
46 capsids can be externalized by heat *in vitro* (Hernando *et al.*, 2000; Carreira *et al.*, 2004;
47
48 Riolobos *et al.*, 2010), but in DNA-filled virions some 2Nt are projected outside the capsid
49
50
51
52
53
54
55
56
57
58
59
60
61
62
63
64
65

1
2
3 (Cotmore and Tattersall, 2007; Plevka *et al.*, 2011; Subramanian *et al.*, 2017) presumably
4 through the fivefold cylinder (Tsao *et al.*, 1991; Agbandje-McKenna *et al.*, 1998). The 2Nt
5 serves as a signal for active nuclear export of mature MVM prior to cell destruction, an
6 activity that may be crucial for successful viral dissemination in tissues (Maroto *et al.*,
7 2004). Additionally, although devoid of recognized import signals, some intracellular
8 exposure-competent 2Nt are required for the incoming virus to initiate infection (Sánchez-
9 Martínez *et al.*, 2012; Castellanos *et al.*, 2013). 2Nt externalization presumably enlarges
10 the capsid pore in the endosome (Sánchez-Martínez *et al.*, 2012), facilitating its cleavage-
11 off VP2 subunits observed in the pH-dependent entry pathway of many parvoviruses
12 (Tullis *et al.*, 1992; Mani *et al.*, 2006; Boisvert *et al.*, 2010; Parrish *et al.*, 2010), a dynamic
13 process leading to 1Nt externalization (Cotmore *et al.*, 1999; Farr *et al.*, 2006; Cotmore
14 and Tattersall, 2014; reviewed in Ros *et al.*, 2017).

15
16
17
18
19
20
21
22
23
24
25
26
27
28
29
30
31
32 In productively infected cells, parvovirus capsid assembly takes place in the nucleus
33 (Hoque *et al.*, 1999; Lombardo *et al.*, 2000), involving orchestrated interactions among capsid
34 subunits. In MVM, assembly begins with the formation of two trimeric intermediates in the
35 cytoplasm at stoichiometric amounts, a homotrimer (3VP2) and a heterotrimer (1VP1/2VP2)
36 (Riolobos *et al.*, 2006). Isolated trimers were nuclear transport competent in permeabilized
37 cells without any other viral component (Riolobos *et al.*, 2010; Gil-Ranedo *et al.*, 2015).
38 Trimers are translocated into the nucleus driven by a structured protein motif (NLM)
39 displaced on the inner capsid surface as an amphipathic beta-strand (Lombardo *et al.*, 2000).
40 Similar non-conventional nuclear transport sequences localized in partially overlapping or
41 contiguous homologous amino acid sequence of the NLM (Valle *et al.*, 2006), were required
42 for nuclear capsid assembly of the human B19 (Pillet *et al.*, 2003), and porcine PPV (Boisvert
43 *et al.*, 2014) parvoviruses. These structured transport motifs may constitute a quality control
44
45
46
47
48
49
50
51
52
53
54
55
56
57
58
59
60
61
62
63
64
65

1
2
3
4 mechanism for the assembly pathway, precluding the nuclear import and assembly of
5
6 misfolded subunits or trimers with unbalanced VP1 content (Lombardo *et al.*, 2000). Within
7
8 the nucleus, the MVM trimers interact through a few residues via hydrophobic and hydrogen
9
10 bonds (Reguera *et al.*, 2004), and must undergo conformational rearrangements to their final
11
12 configuration in the capsid (Riolobos *et al.*, 2006 and 2010). In AAV2, an assembly-
13
14 activating protein (AAP) encoded by the viral cap gene was essential for capsid assembly
15
16 (Sonntag *et al.*, 2010) presumably adapting the conformation of the VP subunits (Naumer *et*
17
18 *al.*, 2012).
19
20
21
22
23

24 The steps of the parvovirus life cycle (gene expression, nuclear translocation of proteins,
25
26 capsid assembly, genome replication and encapsidation) are tightly coupled to the host cell
27
28 cycle progression (Gil-Ranedo *et al.*, 2015). Importantly, parvovirus MVM gene expression
29
30 in synchronous infection occurred at G1/S, implying that transcription does not require a
31
32 previous viral DNA amplification, which indeed occurred later at S/G2 phase (Gil-Ranedo
33
34 *et al.*, 2015). Capsid formation is particularly sensitive to cell cycle regulation, which is
35
36 exerted at the level of non-conventional nuclear transport route(s) accessed by the assembly
37
38 intermediates (Gil-Ranedo *et al.*, 2015). The coupling of parvovirus assembly to the cell
39
40 cycle may largely rely on control of capsid subunits phosphorylation. In MVM infection,
41
42 VP1 and VP2 structural subunits assembled into empty capsids were post-translationally
43
44 modified through a complex and VP-specific pattern of phosphoserine and
45
46 phosphothreonine residues (Maroto *et al.*, 2000). The 3-D structure of virus-like particles
47
48 (VLPs) lacking phosphorylation (Hernando *et al.*, 2000; Riolobos *et al.*, 2010) that
49
50 assembled in the cytoplasm (Riolobos *et al.*, 2010; Yuan and Parris, 2001) indicated that, at
51
52 least for the VP2-only capsid, subunit phosphorylation is not important for icosahedral T=1
53
54
55
56
57
58
59
60
61
62
63
64
65

1
2
3 ordering. However, nuclear transport of the VP2 homotrimer requires cytoplasmic
4 phosphorylation by the Raf-1 kinase (Riolobos *et al*, 2010), although this phosphorylation
5 was not sufficient to explain its cell cycle-regulated transport (Gil-Ranedo *et al.*, 2015). Raf-
6 1 phosphorylation targets serine residues of 2Nt (Maroto *et al.*, 2000 and 2004), but
7 localization of the many other phosphorylation sites in the VP1 and VP2 capsid subunits
8 and their functions in the steps of the viral life cycle are unknown.
9

10
11 In this report, we have further investigated the phosphorylation and Nt configuration of
12 the MVM structural proteins found in assembly intermediates and viral particles. Our focus
13 was mainly on the less-studied VP1 subunits and their involvement in cell cycle-dependent
14 VPs nuclear transport, capsid assembly, and MVM genome packaging. We show that VP1
15 subunits are hyperphosphorylated in cytoplasmic assembly intermediates, but are subjected
16 to an orchestrated dephosphorylation programme during assembly that correlates with
17 changes in Nt configuration. Furthermore, empty and DNA-filled virus particles drastically
18 differed in the phosphorylation status of their VP1 and VP2 protein subunits. These data
19 are integrated into an assembly and viral trafficking unified model of potential general
20 interest to understand the life cycle of icosahedral nuclear viruses.
21
22
23
24
25
26
27
28
29
30
31
32
33
34
35
36
37
38
39
40
41
42
43
44
45
46
47
48
49
50
51
52
53
54
55
56
57
58
59
60
61
62
63
64
65

Materials and Methods

Virus and cell culture.

The prototype (p) strain of the *Protoparvovirus* Minute Virus of Mice (MVMp; Crawford, 1966) was used in this study and referred as MVM. The NB324K simian virus 40-transformed human newborn kidney cell line highly susceptible to the MVM strains (Gardiner and Tattersall, 1983), and a constitutively VPs-expressing stably transfected clone (Gil-Ranedo *et al.*, 2015), were maintained under minimal number of passages in Dulbecco Modified Eagle Medium (DMEM) supplemented with 5% heat-inactivated foetal calf serum (FCS; Gibco BRL). Wherever indicated in the text, infected or transfected cells were synchronized at G1/S with the DNA polymerase- α antagonist aphidicolin, or at G1 upon transfection by density arrest, as described (Gil-Ranedo *et al.*, 2015). Viral stocks used for infections were prepared from large-scale transfection using the pMM984 infectious plasmid (Tattersall and Bratton, 1983), and purified devoid of empty capsids as described (Sánchez-Martínez *et al.*, 2012). Infectious virus titers and reliable plaque sizes were obtained by optimizing previously described plaque assay methods (Tattersall and Bratton, 1983; Rubio *et al.*, 2005) as follows. NB324K cells were dispersed by carefully flushing three times through a 22G needle, and seeded at a density of 2×10^5 cells/P60mm dish. Virus dilutions and cell inoculation (0.25 ml of virus sample per P60mm dish) were performed the next day in complete PBS supplemented with 0.1% FCS. After virus adsorption (1 h at 37 °C under constant shaking) cells were overlaid with 7 ml/P60mm dish of a freshly prepared media composed of DMEM, 10 % FCS, non-essential amino acids, and 0.7% low melting agarose (SeaPlaqueTM Lonza, prepared in ddH₂O). Plaques were developed six days afterwards by

1
2
3 fixing with 10% formaldehyde, and staining with 0.1 % crystal violet prepared in 4 %
4 formaldehyde.
5
6
7
8
9

10 *Flow cytometry.*

11 Cell were fixed, permeabilized, and stained for viral antigens expression and DNA content as
12 described (Gil-Ranedo *et al.*, 2015). Samples were analyzed in a BD Biosciences FACSCanto
13 II Flow Cytometer with the BD FACSDiva (v6.1.2, BD Biosciences) and FlowJo (v9.3
14 TreeStar) softwares.
15
16
17
18
19
20
21
22
23
24
25
26

27 *Plasmids.*

28 A non-replicative genomic clone of the MVMp viral strain (Ramirez *et al.*, 1995; pMVM.WT),
29 and the pMVM.VP1-only and pMVM.VP2-only derived genomic clones constructed by cDNA
30 cloning allowing single expression of each of the structural proteins (Sánchez-Martínez *et al.*,
31 2012), were used in cell transfections. Other plasmids were the pSVtk-VPs expressing the VP1
32 and VP2 capsid proteins of MVMp (Ramirez *et al.*, 1995), and the pSVtk-VPs K153A and
33 pSVtk-VPs L565W plasmids carrying single mutations in the common sequence of both
34 structural proteins (Reguera *et al.*, 2004) that impaired capsid assembly (Riolobos *et al.*, 2006).
35
36
37
38
39
40
41
42
43
44
45
46
47
48

49 *Production of purified radiolabeled viral particles.*

50
51 ³²P-labeled empty capsids and DNA-filled viral particles of MVMp were produced and
52 purified in NB324K cells following a previously described method (Maroto *et al.*, 2000;
53 Santarén *et al.*, 1993) with some modifications. Cells were infected at MOI 10, starved for 4 h
54 in phosphate-free DMEM supplemented with 5 % dialyzed FCS, and labeled from 4 to 42 hpi
55
56
57
58
59
60
61
62
63
64
65

1
2
3
4 in the same medium containing 0.5 mCi per ml of [³²P]orthophosphate carrier free
5
6 (Amersham). Cultures were scraped into the medium supplemented with 0.2 % sodium dodecyl
7
8 sulphate (SDS), proteases (1mM phenylmethylsulfonyl fluoride (PMSF); 10 µg/ml aprotinin;
9
10 10 µg/ml pepstatin; 10 µg/ml leupeptine) and phosphatases (5 mM NaF, 20 mM β-
11
12 glycerophosphate) inhibitors, clumps disaggregated by gentle sonication, and debris removed
13
14 by low speed centrifugation (10,000 x g, 15 min). Homogenates were centrifuged at 15 °C and
15
16 30,000 x g for 18 h in a Sorvall AH627 rotor, through two volumes of a 20 % sucrose cushion
17
18 in 50 mM Tris pH 7.5, 50 mM NaCl, 1 mM EDTA, and 0.2 % SDS. Pellets were resuspended
19
20 in 1 ml per 90 mm dish of 20 mM Tris-HCl pH 7.5, 1 mM EDTA, 0.2 % Sarkosyl, and the
21
22 proteases and phosphatases inhibitors as above, the suspensions adjusted to a density of 1.38
23
24 g/ml in CsCl by refractometry, and centrifuged to equilibrium at 150,000 x g for 24 h and 12
25
26 °C in a Sorvall TFT 80.13 rotor. Fractions with a density corresponding to empty capsids (1.32
27
28 g/ml), and DNA-full virus (1.39-1.41 g/ml), were pooled apart and centrifuged again at the
29
30 same conditions. The ³²P-label distribution in the second round of gradients was determined by
31
32 scintillation counting, fractions of empty and DNA-filled virus extensively dialyzed against
33
34 PBS, and finally concentrated by ultracentrifugation at 100,000x g and 4 °C for 6 h in a SW
35
36 40Ti Beckman rotor.

37
38 To fairly determine the phosphorylation level of the MVM capsid subunits in the viral
39
40 particles (Fig. 5), SDS-PAGE gels containing resolved proteins of purified ³²P-labeled empty
41
42 capsids and DNA-filled virus were equilibrated at room temperature for 15 min in twenty gel-
43
44 volumes of 20 mM Tris-HCl pH 7.5, 10 mM MgCl₂, 5 mM NaCl, and then incubated in two
45
46 gel-volumes with 10 U/ml of DNase I (Promega) for 30 min at 37 °C under shaking. The gel
47
48 was finally fixed in methanol-acetic, dried under vacuum, and exposed for autoradiography to
49
50 X-ray films.
51
52
53
54
55
56
57
58
59
60
61
62
63
64
65

Antibodies

A collection of rabbit and mouse antibodies was used to specifically identify MVM capsid proteins, which included: a rabbit antiserum recognizing unassembled VP1 and VP2 subunits (α -VPs; Gil-Ranedo *et al.*, 2015); a mouse monoclonal antibody recognizing a structured epitope conformed at the 3x axis of the MVM capsid (α -Capsid, B7-MAb; López-Bueno *et al.*, 2003; Kaufmann *et al.*, 2007) but failing to react with unassembled or VP trimeric assembly intermediates (Riolobos *et al.*, 2006; 2010); a rabbit antiserum raised against a 2Nt peptide that recognized mature DNA-filled virus (Maroto *et al.*, 2004); a rabbit antiserum raised against an expressed 1Nt peptide (Cotmore *et al.*, 1999); and a mouse antiserum raised against denatured VP2 purified by SDS-PAGE following a previously described methodology (Gil-Ranedo *et al.*, 2015), which was used for double immunofluorescence in combination with the rabbit α -2Nt and α -1Nt antibodies (α -VPs, Fig. 2 to 4).

Immunological analyses.

Double-labeled indirect immunofluorescence (IF) was performed in cells fixed with 4% paraformaldehyde buffered at pH 7.0 following previously described methods (Gil-Ranedo *et al.*, 2015; Lombardo *et al.*, 2002; Maroto *et al.*, 2004). Phenotypes were visualized by epifluorescence in a Zeiss Axiovert2000 inverted microscope coupled to a SPOT RT Slider digital camera and MetaVue 5.07 software, and images were taken in a Zeiss LSM 710 Laser Scanning confocal microscope and ZEN 2008 software. For western-blot analysis, protein samples resolved in 8 % SDS-PAGE and electro-blotted to nitrocellulose membranes were probed with the indicated antisera, developed with chemiluminescence (Thermo scientific), and exposure to X-ray films.

1
2
3
4
5
6 *Isolation of radiolabeled assemblies.*

7
8 NB324K cells stably expressing VPs proteins were arrested at G1/S by isoleucine
9 deprivation and aphidicolin as described (Gil-Ranedo *et al.*, 2015), and labeled for 4 h within
10 the arrest with 200 $\mu\text{Ci/ml}$ of ^{35}S -methionine (Pro-mixTM, Amersham) in methionine-free
11 medium, or with 2 mCi/ml of carrier-free ^{32}P -orthophosphate (Amersham) in phosphate-free
12 medium. At the end of the labelling periods cells were detached with trypsin and disrupted in
13 50 mM Tris-HCl pH 7.5, 10 mM NaCl in a cooled water bath sonicator. Lysates cleared by
14 centrifugation at 15000 x g and 4 °C for 15 min in a bench-top centrifuge were subjected to
15 immune-precipitation with the indicated antibodies bound to protein A-Sepharose in 50 mM
16 Tris-HCl pH 7.5, 10 mM NaCl and proteases and phosphatase inhibitors (Calbiochem;
17 Riolobos *et al.*, 2010), under native (0.1 % Nonidet P-40) or denaturing (0.5 % SDS)
18 conditions, and the precipitated boiled in Laemmli buffer prior SDS-PAGE and
19 autoradiography.
20
21
22
23
24
25
26
27
28
29
30
31
32
33
34
35
36
37
38
39

40 *2D phosphopeptides analysis.*

41
42 A previously described methodology was followed (Maroto *et al.*, 2000; Riolobos *et al.*, 2010).
43 In brief, the structural proteins of ^{32}P -radiolabelled purified empty capsids and DNA-filled viral
44 particles were resolved by 8 % SDS-PAGE, blotted to nitrocellulose membranes, and exposed
45 for autoradiography. The phospho-labelled VP1 and VP2 proteins were cut-off from the
46 membranes and subjected to 2-D tryptic phosphopeptide analysis by digestion with N-tosyl-L-
47 phenylalanine chloromethyl ketone (TPCK)-trypsin (sequencing grade, Boehringer). The
48 resulting phosphopeptides were 2-D resolved in 20x20 cm TLC plates (Merck, Darmstadt,
49 Germany), and the plates exposed to a radioanalytic imaging system (Fujix BAS 1000, Fuji) for
50
51
52
53
54
55
56
57
58
59
60
61
62
63
64
65

1
2
3 the indicated periods of time. The optical densities of the recorded phosphopeptide spots, as
4
5 well as the phosphoprotein bands obtained in the autoradiography films, were determined with
6
7 a GS-900TM-Calibrated Densitometer (Bio-RadLaboratories, Hercules, California, USA).
8
9
10
11
12
13
14
15
16
17
18
19
20
21
22
23
24
25
26
27
28
29
30
31
32
33
34
35
36
37
38
39
40
41
42
43
44
45
46
47
48
49
50
51
52
53
54
55
56
57
58
59
60
61
62
63
64
65

Results

The protein subunits of MVM trimeric capsid assembly intermediates are unevenly phosphorylated.

At early stages of the MVM assembly pathway, the S phase-coupled nuclear translocation of trimeric intermediates required VPs phosphorylation by Raf-1 (Riolobos *et al.*, 2010), although a significant change in the VP2 phosphorylation pattern between quiescent and proliferating cells was not evident (Gil-Ranedo *et al.*, 2015). To analyze a possible role of VP1 phosphorylation in this process, the VP1/VP2 phosphorylation ratio in the trimers was studied prior to nuclear transport. We used VPs-expressing transfected human NB324K cells, which harboured high Raf-1 constitutive activity (Riolobos *et al.*, 2010) and cell cycle dependent VPs transport as happens in infection (Gil-Ranedo *et al.*, 2015). The subcellular distribution of VPs subunits (Fig. 1A) either during growth, arrested at G1/S, or released from the arrest, was consistent with the previously described cell cycle dependence (Gil-Ranedo *et al.*, 2015). Therefore, synchronized cells at G1/S showing VPs retained in the cytoplasm (Fig. 1A, middle panel) were labeled during the arrest with ³⁵S-Met or with ³²P-orthophosphate, cell extracts immunoprecipitated with antibodies recognizing the 1Nt (α -VP1 antibody), or total unfolded VPs subunits (α -VPs antibody) under native or denaturing conditions (see Materials and Methods), and subjected to SDS-PAGE and autoradiography. Whereas denaturing conditions probed the specificity of the antibodies (Fig. 1B, d lanes), immunoprecipitation in native conditions of the ³⁵S-labeled samples showed a 1:5 ratio of VP1:VP2 subunits in the assemblies, their approximate stoichiometry of synthesis (Riolobos *et al.*, 2006), when using the α -VPs antibody, but a ratio close to 1:2 when the α -VP1 antibody was used (Fig. 1B, n lanes; Fig. 1C). This

1
2
3 result indicated that the VP1 subunits assemble into a cytoplasmic 1VP1:2VP2
4 heterotrimer in G1/S arrested cells. The ³²P-labeled immunoprecipitates showed that newly
5 synthesized VP1 and VP2 proteins accumulating in the cytoplasm were phosphorylated
6 (Fig. 1B, d lanes). Importantly, the denaturing conditions of immunoprecipitation allowed
7 resolution of the phosphorylated proteins at a VP1:VP2 ratio close to 1.0 (Fig. 1B, C). In
8 respect to their ratio of synthesis shown above, this result indicated that, on average, VP1
9 subunits assembled in cytoplasmic trimers harbored a phosphorylation level close to
10 fivefold higher than that of the VP2 subunits. Whether the VP2 subunits assembled in
11 homo- (3VP2) and the hetero- (1VP1/2VP2) trimers differed in phosphorylation level
12 could not be discerned.

13
14
15
16
17
18
19
20
21
22
23
24
25
26
27
28 *Exposure of VP N-terminal domains in cytoplasmic assembly intermediates.*
29

30 To get further insights into MVM assembly, we assessed changes in the configuration of
31 the capsid subunits throughout the process by testing the accessibility of the VP1 (1Nt) and
32 VP2 (2Nt) N-terminal domains to specific antibodies in cytoplasmic and nuclear assembly
33 intermediates. It was previously shown that nuclear transport of VPs in transfected and
34 infected NB324K cells was inhibited when subjected to density arrest contacts by a VP2-
35 driven mechanism (Gil-Ranedo *et al.*, 2015). We therefore studied whether the Nt
36 domains, carrying transport signals (see above), may contribute to this cell cycle-dependent
37 mechanism. For this, we used a viral genomic plasmid (pMVM), and derived genomic
38 constructs lacking either VP1 or VP2 (Sanchez-Martinez *et al.*, 2012), in transfections
39 under different culture conditions. In pMVM transfections, the 1Nt domain was stained
40 only in the nucleus under normal low cell density, but not in cells showing a cytoplasmic
41 or mixed VPs transport phenotype at high density (Fig. 2 upper panels). In the absence of
42 VP2 subunits though (pMVMVP1-only transfections), the 1Nt domain was efficiently
43
44
45
46
47
48
49
50
51
52
53
54
55
56
57
58
59
60
61
62
63
64
65

1
2
3
4 stained in the nucleus of cells grown to low and high density (Fig. 2, bottom panels). The
5
6 2Nt domain became similarly accessible to specific antibodies in the nucleus of pMVM
7
8 and pMVMVP2-only transfected cells cultured at low density, denoting the production of
9
10 DNA-filled viral particles, but not in singly expressed nuclear VP1 subunits albeit they
11
12 contain the 2Nt amino acids sequence (Fig. 2, left panels). However, 2Nt was hidden when
13
14 pMVM and pMVMVP2-only transfected cells grown to confluence showed significant
15
16 cytoplasmic retention of VPs (Fig. 2, right panels), consistent with the impaired capsid
17
18 assembly and virus maturation under this culture condition (Gil-Ranedo *et al.*, 2015).
19
20
21 These results demonstrated that: (i) the Nt domains were not accessible to antibodies in the
22
23 cytoplasm; (ii) the nuclear 1Nt exposure required low cell density in wt, but not in VP1-
24
25 only transfections; and (iii) the 2Nt was only exposed in the nucleus of productively
26
27 transfected cells. Therefore, the previously recognized VP2 mediated cell cycle regulation
28
29 of MVM assembly (Gil-Ranedo *et al.*, 2015) involves the masking of the 1Nt and 2Nt
30
31 domains by the VP2 subunits.
32
33
34
35
36

37 *Differential Nt exposures in nuclear MVM capsid assembly intermediates.*

38
39
40 To further investigate the nuclear stages of the MVM assembly process, we analyzed the
41
42 exposure of 1Nt and 2Nt in trimers and larger VP oligomers accumulated in the nucleus
43
44 prior to viral particles formation. For this, we used the VP-expressing wt (pSVtk-VPs;
45
46 Sánchez-Martínez *et al.*, 2012), and the derivative K153A and L565W mutant plasmids
47
48 lacking inter-subunits contacts (Reguera *et al.*, 2004), which yielded trimers (8.9 S) and
49
50 uncharacterized larger (approximate 30 S) nuclear subviral assemblies respectively
51
52 (Riolobos *et al.*, 2006). A preliminary study was required to establish culture conditions
53
54 supporting cell cycle control of VPs nuclear transport in transiently transfected cells. As
55
56 shown in Fig. 3A, pSVtk-VPs transfected cells seeded at low density showed efficient
57
58
59
60
61
62
63
64
65

1
2
3 nuclear capsid formation (growing cultures), but culturing at high density led to a
4 significant cycle arrest at G1, marked impairment of VPs nuclear transport, and capsid
5 assembly restricted to a weak punctuated cytoplasmic phenotype (Fig. 3A, density arrest).
6 Under these satisfactory culture conditions, transfections at low cell density (Fig. 3B, left
7 growing panels) displayed uniform (wt-VPs, and K153A) or punctuated (L565W) nuclear
8 VPs staining, as previously reported (Riolobos *et al.*, 2006). The wt and both mutant
9 assemblies clearly exposed the 1Nt domain in the nucleus (Fig. 3B, left panels). At high
10 cell density though the nuclear accumulation of wt and mutant VPs subunits was severely
11 impaired, as above, and the accessibility of their 1Nt domains significantly declined even
12 inside the nucleus, suggesting structural masking (Fig. 3B, right panels). Under this
13 culture condition of inhibited VPs transport, instead of a fine punctuated phenotype, the
14 L565W mutant yielded large cytoplasmic circles and dots reassembling ubiquitin-
15 conjugated aggregates found in some assembly incompetent VP1/ Δ VP2 deletion mutants
16 (Lombardo *et al.*, 2002). The 2Nt domain was not accessible in any assembly intermediate
17 regardless of the subcellular accumulation, consistent with the absence in these plasmids of
18 nonstructural proteins essential for genome replication and 2Nt exposure in mature virus
19 (Maroto *et al.*, 2004) and packaging intermediates (Cotmore and Tattersall, 2005). These
20 experiments: (i) confirmed that the Nt domains are not accessible to antibodies in the
21 cytoplasmic assembly intermediates; (ii) demonstrated that trimers undergo a
22 conformational shift upon nuclear translocation exposing 1Nt in the heterotrimer, but
23 keeping 2Nt hidden in both types of trimers; and (iii) further showed that trimers and larger
24 subviral assembly intermediates accumulated in the nucleus maintain the 1Nt exposed.

25
26
27
28
29
30
31
32
33
34
35
36
37
38
39
40
41
42
43
44
45
46
47
48
49
50
51
52
53
54
55
56
57
58
59 *Exposure of the 1Nt and 2Nt domains throughout the MVM synchronous infection cycle.*
60
61
62
63
64
65

1
2
3
4 To determine whether the MVM assembly results obtained in transfection studies were
5 supported in the context of natural infection, we analyzed the exposure of the Nt domains
6 along the VPs subcellular distribution and assembly in a synchronous infection cycle (Fig.
7 4). NB324K cells infected by purified MVM (MOI 5), showed weak signals from the input
8 viral particles while under G1/S aphidicolin arrest (Fig. 4; 0 hpa panels). As cells released
9 from the arrest moved into S phase (Fig. 4A; 6 hpa), the expressed VPs filled the
10 cytoplasm and underwent simultaneous nuclear translocation to a mixed phenotype (Fig.
11 4B; 6 hpa panels), with weak capsid and 1Nt staining confined to the nucleus in less than 8
12 % of the cells. When the S /G2 phases boundary was reached and cells showed marked
13 nuclear accumulation of VPs (Fig. 4; 8 hpa panels), a significant increase in the capsid and
14 1Nt nuclear staining was demonstrated, whereas weak 2Nt nuclear staining became first
15 evident in a low percentage of cells. At late times of the infection cycle, when the bulk of
16 viral genome replication takes place (Gil-Ranedo *et al.*, 2015), infected cells showed a
17 patent S/G2 arrest as compared to the predominant G2/G1 phase of uninfected cells (Fig.
18 4A; 10 hpa), and most nuclei stained intensely with all four antibodies (Fig. 4B; 10 hpa
19 panels). This experiment showed that during infection, as in transfection: (i) the 1Nt and
20 2Nt domains are not exposed in cytoplasmic protein subunits and assembly intermediates;
21 (ii) the VPs translocation into the nucleus at mid S phase led to 1Nt exposure coinciding
22 with the rise of capsid assembly; (iii) upon VPs nuclear accumulation not only capsid but
23 also 1Nt staining remained positive throughout the final stages of the infection cycle; and
24 (iv) the 2Nt was newly exposed at times of virus genome replication and maturation.

25
26
27
28
29
30
31
32
33
34
35
36
37
38
39
40
41
42
43
44
45
46
47
48
49
50
51
52
53
54
55
56
57
58
59
60
61
62
63
64
65
Empty and DNA-filled viral particles drastically differ in the phosphorylation level of their VPI subunits.

1
2
3
4 Following the assembly pathway VPs oligomers form the MVM particles in the nucleus
5
6 (Lombardo *et al.*, 2000; Riolobos *et al.*, 2006). The MVM empty capsid assembled in
7
8 NB324K cells had protein subunits modified in a specific 2-D pattern of Ser/Thr
9
10 phosphorylation (Maroto *et al.*, 2000). To investigate a possible role of VPs
11
12 phosphorylation in MVM maturation, the phosphorylation status of the VP1 and VP2
13
14 subunits assembled in *in vivo* ³²P-labelled empty capsid and DNA-filled virus highly
15
16 purified from NB324K cells at 40 hpi (see Materials and Methods) was carefully re-
17
18 examined. Empty capsids harbored a VP1:VP2 phosphorylation ratio close to their 1:5
19
20 stoichiometry of synthesis (Fig. 5). However, this ratio was at least fourfold lower in the
21
22 DNA-filled virus purified from two independent experiments, as the viral VP1 subunits
23
24 consistently showed barely detectable phosphorylation (Fig. 5; Exp #1 and #2). To rule out
25
26 deficient transfer to filters of putative highly phosphorylated VP1 protein species, the
27
28 actual phosphorylation level of the VPs subunits assembled in both types of viral particles
29
30 was determined inside the resolving gels. An in gel extensive removal of the abundant
31
32 phospholabel from the ssDNA genome backbone was required to visualize the virus
33
34 phosphoproteins (see Materials and Methods). As shown in Fig. 5 (Exp#2; right panel), the
35
36 autoradiography of gels subjected to this treatment confirmed the virtually
37
38 unphosphorylated status of the VP1 subunits assembled in the DNA-filled virus.
39
40
41
42
43
44
45

46
47 *Pattern of VP2 phosphorylation and dephosphorylation in MVM particles.*
48

49 Unlike VP1, the VP2 subunits of purified viruses remained significantly phosphorylated
50
51 (Fig. 5), prompting us to study in greater detail whether viral genome packaging involves
52
53 alteration of the VP2 phosphorylation pattern. For this, the VP2 protein subunits of ³²P-
54
55 labelled MVM empty capsids and DNA-filled viruses purified as above were subjected to
56
57 2D tryptic phosphopeptides analysis. As shown in Fig. 6 (*upper left panel*), the VP2
58
59
60
61
62
63
64
65

1
2
3 subunits of empty capsids showed the characteristic 2-D phosphopeptides map previously
4 reported (Maroto *et al.*, 2000). Albeit the limited availability of ^{32}P counts in the proteins
5 of highly purified virus samples, the overall 2D phosphopeptides pattern was fairly
6 preserved in the virus VP2 subunits. However, one of the main VP2 capsid
7 phosphopeptides, termed I in the original described map (Maroto *et al.*, 2000), showed a
8 relative phosphorylation level significantly lower in the virus ^{32}P -fingerprints (Fig 6, *lower*
9 *left panel*). This selective under-representation of phosphopeptide I was consistently
10 observed in three independent virus purifications (data not shown).
11
12
13
14
15
16
17
18
19
20
21
22
23

24 Finally, we focused on the phosphorylation status of the virus-specific VP3 subunits,
25 a protein resulting from the 2Nt-cleavage off VP2 protein as the incoming virus traffic
26 through the endosome (Sánchez-Martínez *et al.*, 2012; and references therein).
27 Remarkably, an absolute dephosphorylated stage was observed for the VP3 protein blotted
28 to filters (Fig. 5), as well as for the protein analyzed inside the resolving gels (Fig. 5, *lower*
29 *right panel*). The lack of phospholabel in VP3 was consistent with the phosphoserine
30 residues that mapped to the 2Nt (Maroto *et al.*, 2000), and with the severe
31 dephosphorylation of peptide I in the virus VP2 (Fig. 6). In conclusion, as only the
32 uncleaved virus VP2 subunits maintained most VP2 phosphopeptides, the phosphorylation
33 level of the protein coat in DNA-filled virus is markedly lower than that of the empty
34 capsid.
35
36
37
38
39
40
41
42
43
44
45
46
47
48
49
50
51
52
53
54
55
56
57
58
59
60
61
62
63
64
65

Discussion

Nuclear icosahedral DNA viruses of animals share the common need to protect their genome during cytoplasmic trafficking until its delivery into the nucleus, and to orchestrate an assembly pathway of asymmetric structural subunits that must translocate across the nuclear envelope to package the genome. However, their strategies, cellular effectors, and molecular mechanisms are widely diverse. The life cycle of the ssDNA viruses of the *Parvoviridae* proceeds through highly efficient concatenated processes that are tightly dependent on cell physiology, which complicates its molecular characterization. We found necessary the use of mutants halting the assembly process at specific stages (Lombardo *et al.*, 2000, 2002; Riolobos *et al.*, 2006), synchronization of infected and transfected cells (Gil-Ranedo *et al.*, 2015), and 2-D high resolution of capsid subunits phosphorylation patterns (Maroto *et al.*, 2000, 2004; Riolobos *et al.*, 2010), to interpret parvovirus MVM assembly data. In this report, these methodologies were used to search additional configuration and phosphorylation features of assembly intermediates and MVM particles. To facilitate understanding, our major findings have been integrated into the model depicted in Fig. 7, which is discussed below.

Role of Nt exposure and phosphorylation in the cell cycle-regulated nuclear transport of parvovirus capsid subunits.

Studying cytoplasmic VPs assembly in transfected cells arrested in G1 by contact inhibition is relevant to what happens in a productive MVM infection, as VPs expression occurs soon after release of the G1/S arrest, several hours prior viral genome replication, and moreover infected cells subjected to cycle arrest at G1 showed significant VPs expression (Gil-Ranedo *et al.*, 2015). The MVM capsid subunits expressed in G1/S

1
2
3
4 synchronous cells were isolated as cytoplasmic homo- 3VP2, and hetero- 2VP2:1VP1
5
6 trimers (Fig. 1), consistent with the composition of these early assembly intermediates
7
8 obtained by chemical cross-linking and sedimentation (Riolobos *et al.*, 2006). In the
9
10 configuration adopted in the cytoplasm, the Nt domains of the trimeric subunits were not
11
12 accessible to antibodies in transfected or infected cells (Fig. 2-4), suggesting their
13
14 structural and functional masking. As 1Nt harbors a consensus NLS, which suffices for the
15
16 nuclear transport of singly expressed VP1 proteins (Lombardo *et al.*, 2002; Vihinen-Ranta
17
18 *et al.*, 2002), its functional inactivation must be accounted for by the cytoplasmic
19
20 interaction of VP1/VP2 subunits in the heterotrimer. This masking would also explain why
21
22 1Nt is incompetent to drive the cell cycle dependent VPs transport (Gil-Ranedo *et al.*,
23
24 2015, and Fig. 2).

25
26
27
28
29
30
31 In the restricted conformational and functional cytoplasmic 1Nt exposure,
32
33 phosphorylation may play a role, as the phosphorylation level of the VP1 subunits in the
34
35 cytoplasmic heterotrimers was five fold higher than that of the VP2 (Fig. 1B, C). In
36
37 purified empty capsids, VP1 was phosphorylated at multiple Ser and Thr residues (Maroto
38
39 *et al.*, 2000), but the localization of these residues, and their relationship with the
40
41 cytoplasmic hyper-phosphorylation of the heterotrimer, remains to be characterized. Inside
42
43 the nucleus VP1 subunits are subjected to an orchestrated dephosphorylation programme
44
45 during subsequent steps of the viral life cycle (Fig. 5). Interestingly, after nuclear
46
47 translocation, heterotrimers displayed an exposed 1Nt (Fig. 3 and 4), a conformation
48
49 switch that may be coordinated by dephosphorylation and confer directionality to the
50
51 assembly pathway (Fig. 7).
52
53
54
55
56
57
58
59
60
61
62
63
64
65

1
2
3
4 In contrast, the 2Nt domain was hidden (Fig. 2 to 4), and remained at similar
5 phosphorylation levels (Gil-Ranedo *et al.*, 2015), in both cytoplasmic and nuclear trimers.
6
7
8 The inaccessibility of 2Nt during during nuclear import may structurally mask its export
9 activity (Maroto *et al.*, 2004). It is also possible that this hidden 2Nt conformation is
10 regulated by phosphorylation, as a Raf-1 kinase mediated phosphorylation, which targeted
11 three serine residues located within 2Nt, was strictly required for VP2 nuclear import
12 (Riolobos *et al.*, 2010). Therefore, the phosphorylation status of the cytoplasmic trimers
13 may impose a configuration in which both 1Nt and 2Nt are hidden and functionally
14 inactive, and inter-trimer contacts blocked to avoid premature capsid assembly. In response
15 to other cellular signals or factors yet to be characterized, trimers with proper folding of the
16 NLM (Lombardo *et al.*, 2000) would access a non-conventional transport route, driving
17 VPs into the nucleus via a cell cycle-coupled mechanism (Gil-Ranedo *et al.*, 2015).
18
19
20
21
22
23
24
25
26
27
28
29
30
31

32 *Capsid subunits configuration and phosphorylation in nuclear assembly and virus*
33 *maturation.*
34
35
36

37 This study suggests that the parvovirus assembly pathway increases complexity inside the
38 nucleus, as it may be illustrated by the 1Nt exposure. Although the 1Nt is concealed within
39 the coat of purified parvovirus viral particles inaccessible to antibodies or proteases *in vitro*
40 (Cotmore *et al.*, 1999; Hernando *et al.*, 2000; Maroto *et al.*, 2004; Mani *et al.*, 2006; Popa-
41 Wagner *et al.*, 2012; Venkatakrishnan *et al.*, 2013), an important 1Nt exposure was
42 observed in the nuclei of infected and transfected cells expressing trimers and larger
43 assembly intermediates (Fig. 2 to 4). Interestingly, nuclear 1Nt nuclear staining was
44 particularly intense at late times of the synchronous infection (Fig. 4). In the absence of
45 evidences for procapsids or characterized large subviral assemblies bearing exposed 1Nt,
46 the significance of the maintained nuclear 1Nt staining remains uncertain.
47
48
49
50
51
52
53
54
55
56
57
58
59
60
61
62
63
64
65

1
2
3
4 During MVM maturation, the DNA-filled virus lacked all the VP1 phosphorylation sites
5
6 (Fig. 5) and one major VP2 phosphopeptide (Fig. 6) found in the empty capsid. This
7
8 disparate phosphorylation status between the two major nuclear viral particles may suggest
9
10 a role of phosphates in viral genome packaging. The most widely accepted model
11
12 delineates parvovirus maturation via an helicase-mediated pumping of the ssDNA genome
13
14 into preformed capsids through a fivefold pore (King *et al.*, 2001; Cotmore and Tattersall,
15
16 2005; Plevka *et al.*, 2011). Fitting our data with this model might suggest that the
17
18 packaging machinery select for a subpopulation of empty capsids harboring
19
20 dephosphorylated VP1 subunits, or that drastic VPs dephosphorylation accompanies viral
21
22 genome encapsidation. The removal of phosphate substituents from VP1 subunits, and a
23
24 precise VP2 phosphorylation status with 2Nt exposure, may be required for specific
25
26 packaging of the parvovirus negatively charged ssDNA genome. Further research
27
28 addressing the phosphorylation of large VPs complexes and viral particles, and their viral
29
30 ssDNA specific interactions, will be required to understand the complex nuclear events
31
32 regulating parvovirus assembly and maturation.
33
34
35
36
37
38

39
40 *Phosphates and Nt domains in viral trafficking.*
41

42 The routing signals mapped in 1Nt and 2Nt led us to propose that the mature MVM would
43
44 alternatively expose these flexible domains for trafficking (Maroto *et al.*, 2004), a concept
45
46 subsequently extended to other parvoviruses (Popa-Wagner *et al.*, 2012; Boisvert *et al.*,
47
48 2014). Consistently with this view, VP2-Nt became exposed only at late times of the
49
50 infection cycle (Fig. 4), suggesting that its function is restricted to the traffic of mature
51
52 virus. The exposure and phosphorylation of 2Nt may thus be relevant to both viral import
53
54 and export. Indeed, 2Nt plays, as 1Nt, an essential role for the MVM infectious entry
55
56 pathway (see Introduction). In virus particles purified from transformed NB324K cells, 2Nt
57
58
59
60
61
62
63
64
65

1
2
3 was heavily phosphorylated (Maroto *et al.*, 2000), but during cell entry most terminal
4 domains are cleaved-off VP2 in the endosome (Sánchez-Martínez *et al.*, 2012, and
5 references therein), and this study shows that the resulting VP3 subunits are, as with VP1,
6 virtually unphosphorylated (Fig. 5). This result raises issue about the actual
7 phosphorylation status of the remaining VP2 subunits in post-endosomal incoming virus
8 particles. Although the VP2 of total virus lacked, in respect to empty capsid, only the
9 phosphorylation site(s) of phosphopeptide I (Fig. 6), we did not compare the
10 phosphorylation status of VP2 in virus purified from the medium and different cellular
11 compartments. Regardless of this uncertainty about VP2, the post-endosomal viral
12 particles routing to the nucleus have a very low or completely dephosphorylated status, a
13 chemical feature that may be required for successful nuclear genome delivery.
14
15
16
17
18
19
20
21
22
23
24
25
26
27
28
29
30

31 The role that capsid phosphorylation plays in parvovirus egress from the nucleus, and
32 from other cellular compartments, is less understood. In NB324K cells, the 2Nt of the
33 MVMp strain was phosphorylated by cytoplasmic Raf-1 kinase (Riolobos *et al.*, 2010), and
34 this modification greatly facilitated viral nuclear egress (Maroto *et al.*, 2004). However, in
35 A9 mouse fibroblasts expressing low Raf-1 activity (Riolobos *et al.*, 2010), MVMp nuclear
36 egress operated by an NS2-CRM1 mediated export pathway (Eichwald *et al.*, 2002; Miller
37 and Pintel, 2002; Engelsma *et al.*, 2008), which paradoxically benefited from mutations
38 inactivating the 2Nt serine phosphorylation sites (Maroto *et al.*, 2004). It was recently
39 reported that lambda phosphatase-sensitive negative charges exposed on the MVMp capsid
40 surface at sites unrelated to 2Nt phosphoserines were enriched in virus particles with
41 nuclear export potential in A9 cells (Wolfsberg *et al.*, 2016). Although further research on
42 the nature and protein distribution of these charges is required to correlate them with NS2
43
44
45
46
47
48
49
50
51
52
53
54
55
56
57
58
59
60
61
62
63
64
65

1
2
3 functions and our phosphorylation studies, the overall data are consistent with a 2Nt
4 phosphorylation-independent nuclear export route in A9 cells. Interestingly, when
5
6 challenging the MVMi strain by a passive neutralizing polyclonal therapy in mice, viruses
7
8 that emerged after evading the immune pressure carried mutations located exclusively
9
10 within the NS2-CRM1 binding domain, and these mutations increased NS2-CRM1 binding
11
12 affinity and enhanced MVMi egress in NB324K cells (Lopez-Bueno *et al.*, 2004).
13
14 Therefore, the available information from different experimental systems supports that the
15
16 NS2- and 2Nt- mediated routes of viral nuclear export are mechanistically linked in a cell
17
18 type-dependent manner. This connection may regulate virus spread and fitness in tissues.
19
20
21
22
23
24
25
26
27

28 **Conclusions**

29
30
31 This study shows that specific phosphorylations and changes in the conformation of the N-
32
33 terminal domains of capsid subunits may contribute to the fine-tuned cell cycle coupling of
34
35 parvovirus assembly, genome encapsidation, and viral trafficking. While cytoplasmic
36
37 trimers and their transport regulation could be characterized, inside the nucleus the
38
39 assembly pathway involved differential phosphorylation and configuration of multiple
40
41 assembly intermediates and viral particles, a complexity challenging our understanding of
42
43 the maturation process of these small viruses. Our study may provide important
44
45 implications for the assembly of other nuclear icosahedral viruses, in particular those
46
47 encoding protein subunits undergoing post-translational phosphorylation. It also points
48
49 toward a network of cell cycle regulatory signals and factors that acting at the level of
50
51 protein phosphorylation may become potential targets for wide antiviral interventions.
52
53
54
55
56
57
58

59 **Acknowledgments**

60
61
62
63
64
65

1
2
3 JG-R, EH, and NV equally contributed to this work. We thank P. Tattersall (Yale, CT) for
4 providing the pMVM infectious plasmid and the VP1-specific polyclonal antibody. This
5 article is in the memory of Juan Fernandez Santarén and his unique legacy of 2-D resolved
6 proteins.
7
8
9

10 11 12 **Funding Information**

13 This work was supported by the grants SAF2011-29403 (Spanish Ministerio de Ciencia e
14 Innovación), SAF2015-68522-P-MINECO/FEDER, UE (Spanish Ministerio de Economía y
15 Competitividad), and S2013/ABI-2906-FEDER (Comunidad de Madrid), to JMA, and by
16 institutional grants from the Fundación Ramón Areces and Banco Santander to the Centro de
17 Biología Molecular Severo Ochoa (CSIC-UAM).
18
19
20
21
22
23
24
25
26

27 **References**

- 28 Agbandje-McKenna, M., A. L. Llamas-Saiz, F. Wang, P. Tattersall, and M. G.
29 Rossmann. 1998. Functional implications of the structure of the murine parvovirus,
30 minute virus of mice. *Structure* 6:1369–1381.
31
32 Bjorn-Patrick, M., and P. Roy. 2016. Cellular casein kinase 2 and protein phosphatase
33 2A modulate replication site assembly of bluetongue virus. *J. Biol. Chem.* 291: 14566-
34 14574.
35
36 Boisvert, M., Bouchard-Lévesque, V., Fernandes, S., and P. Tijssen. 2014. Classic
37 nuclear localization signals and a novel nuclear localization motif are required for nuclear
38 transport of porcine parvovirus. *J. Virol.* 88: 11748-11759.
39
40 Boisvert, M., Fernandes, S., and P. Tijssen. 2010. Multiple pathways involved in
41 porcine parvovirus cellular entry and trafficking toward the nucleus. *J. Virol.* 84: 7782-92.
42
43 Brownstein, D. G., A. L. Smith, R. O. Jacoby, E. A. Johnson, G. Hansen, and P.
44 Tattersall. 1991. Pathogenesis of infection with a virulent allotropic variant of minute
45 virus of mice and regulation by host genotype. *Lab. Invest.* 65:357–363.
46
47 Carreira, A., Menendez, M., Reguera, J., Almendral, J.M. and M. G. Mateu. 2004. In
48 vitro disassembly of a parvovirus capsid and effect on capsid stability of heterologous
49 peptide insertions in surface loops. *J. Biol. Chem.* 279: 6517-6525.
50
51
52
53
54
55
56
57
58
59
60
61
62
63
64
65

1
2
3
4 Castellanos, M., Pérez, R., Rodríguez-Huete, A., Grueso, E., Almendral, J.M, and M. G.
5 Mateu. 2013. A slender tract of glycines is required for translocation of protein VP2 N-
6 terminal domain through the parvovirus MVM capsid channel to initiate infection.
7 *Biochem. Journal* 455: 87-94.

8
9
10 Cotmore, S., Agbandje-McKenna, M., Chiorini, J.A., Mukha, D.V., Pintel, D.J., Qiu,
11 J.M., Soderlund-Venermo, M., Tattersall, P., Tijssen, P., Gatherer, D., and A. J.
12 Davisonet. 2014. The family Parvoviridae. *Arch Virol.* 159:1239-1247.

13
14 Cotmore, S.F., D'Abramo. A.M. Jr., Ticknor, C.M., and P. Tattersall. 1999. Controlled
15 conformational transitions in the MVM virion expose the VP1 N-terminus and viral
16 genome without particle disassembly. *Virology* 254: 169-181.

17
18 Cotmore, S.F., and P. Tattersall. 2005. Encapsidation of minute virus of mice DNA:
19 aspects of the translocation mechanism revealed by the structure of partially packaged
20 genomes. *Virology* 336: 100–112.

21
22 Cotmore, S.F., and P. Tattersall. 2007. Parvoviral host range and cell entry mechanisms.
23 *Adv. Virus Res.* 70: 183-232.

24
25 Cotmore, S.F., and P. Tattersall. 2014. Parvoviruses: small does not mean simple. *Annu.*
26 *Rev. Virol.* 1: 517-537.

27
28 Crawford, L. V. 1966. A minute virus of mice. *Virology* 29:605-612.

29
30 Eichwald V, Daeffler L, Klein M, Rommelaere J, and N. Salomé. 2002. The NS2
31 proteins of parvovirus minute virus of mice are required for efficient nuclear egress of
32 progeny virions in mouse cells. *J. Virol.* 76:10307–10319.

33
34 Engelsma, D., Valle, N., Fish, A., Salomé, N., Almendral, J.M., and M. Fornerod. 2008.
35 A supraphysiological nuclear export signal is required for parvovirus nuclear export. *Mol.*
36 *Biol. Cell* 19: 2544–2552.

37
38 Farr, G.A., Cotmore, S.F., and P. Tattersall. 2006. VP2 cleavage and the leucine ring at
39 the base of the fivefold cylinder control pH-dependent externalization of both the VP1 N
40 terminus and the genome of minute virus of mice. *J. Virol.* 80: 161–171.

41
42 Farr, G.A., Zhang, L., and P. Tattersall. 2005. Parvoviral virions deploy a capsid-
43 tethered lipolytic enzyme to breach the endosomal membrane during cell entry. *Proc. Natl.*
44 *Acad. Sci. USA* 102: 17148-17153.

1
2
3
4 Gardiner E.M., and P. Tattersall. 1988. Mapping of the fibrotropic and lymphotropic
5 host range determinants of the parvovirus minute virus of mice. *J. Virol.* 62: 2605–2613.
6

7
8 Gil-Ranedo, J., Hernando, E., Riolobos, L., Dominguez, C., Kann, M., and Almendral,
9 J.M. 2015. The mammalian cell cycle regulates parvovirus nuclear capsid assembly. *PLoS*
10 *Pathogens.* 11(6):e1004920.
11

12
13 Gurda, B. L., Parent, K. N., Bladek, H., Sinkovits, R. S., DiMattia, M. A., Rence, C.,
14 Castro, A., McKenna, R., Olson, N., Brown, K., Baker, T. S., and M. Agbandje-McKenna.
15 2010. Human bocavirus capsid structure: insights into the structural repertoire of the
16 parvoviridae. *J. Virol.* 84: 5880-9.
17
18

19
20 Hernando, E., Llamas-Saiz, A.L., Foces-Foces, C., McKenna, R., Portman, I.,
21 Agbandje- McKenna, M., and J.M. Almendral. 2000. Biochemical and physical
22 characterization of parvovirus minute virus of mice virus-like particles. *Virology* 267:
23 299–309.
24
25

26
27 Hoque, M., K.-I. Ishizu, A. Matsumoto, S.-I. Han, F. Arisaka, M. Takayama, K. Suzuki,
28 K. Kato, T. Kanda, H. Watanabe, and H. Handa. 1999. Nuclear transport of the major
29 capsid protein is essential for adeno-associated virus capsid formation. *J. Virol.* 73:7912-
30 7915.
31
32

33
34 Johnson, J. S., Li, C., DiPrimio, N., Weinberg, M. S., McCown, T. J., and R. J.
35 Samulski. 2010. Mutagenesis of adeno-associated virus type 2 capsid protein VP1
36 uncovers new roles for basic amino acids in trafficking and cell-specific transduction. *J.*
37 *Virol.* 84: 8888-902.
38
39

40
41 Kaufmann, B., Chipman, P. R., Kostyuchenko, V. A., Modrow, S., and M.G. Rossmann.
42 2008. Visualization of the externalized VP2 N termini of infectious human parvovirus
43 B19. *J. Virol.* 82: 7306-12.
44
45

46
47 Kaufmann B., Lopez-Bueno A., Mateu M.G., Chipman P.R., Nelson C.D., Parrish,
48 C.R., Almendral, J.M., and M. G. Rossmann. 2007. Minute virus of mice, a parvovirus, in
49 complex with the Fab fragment of a neutralizing monoclonal antibody. *J. Virol.* 81: 9851-
50 9858.
51
52

53
54 Kaufmann, B., Simpson, A. A., and M.G. Rossmann. 2004. The structure of human
55 parvovirus B19. *Proc. Natl. Acad. Sci. U S A.* 101: 11628-33.
56
57
58
59
60
61
62
63
64
65

1
2
3
4 King J.A., Dubielzig R., Grimm S.W., and J.A. Kleinschmidt. 2001. DNA helicase-
5 mediated packaging of adeno-associated virus type 2 genomes into preformed capsids.
6 EMBO J. 20: 3282–3291.
7

8
9 Kontou, M., L. Govindasamy, H.-J. Nam, N. Bryant, A. L. Llamas-Saiz, C. Foces-
10 Foces, E. Hernando, M.-P. Rubio, R. McKenna, J. M. Almendral, and M. Agbandje-
11 McKenna. 2005. Structural determinants of tissue tropism and *in vivo* pathogenicity for
12 the parvovirus minute virus of mice. J. Virol, 79:10931-10943.
13
14

15
16 Mani, B., Baltzer, C., Valle, N., Almendral, J. M., Kempf, C., and C. Ros. 2006. Low
17 pH-dependent endosomal processing of the incoming parvovirus minute virus of mice
18 virion leads to externalization of the VP1 N-terminal sequence (N-VP1), N-VP2 cleavage,
19 and uncoating of the full-length genome. J. Virol. 80: 1015-24.
20
21

22
23 Lombardo, E., J.C., Ramírez, M. Agbandje-Mckenna, and J.M. Almendral. 2000. A β -
24 stranded motif drives capsid proteins oligomers of the parvovirus minute virus of mice
25 into the nucleus for viral assembly. J. Virol. 74:3804-3814.
26
27

28
29 Lombardo, E., Ramírez, J.C., García, J., and J.M. Almendral. 2002. Complementary
30 roles of multiple nuclear targeting signals in the capsid proteins of the parvovirus minute
31 virus of mice during assembly and onset of infection. J. Virol. 76: 7049-7059.
32
33

34
35 Lopez-Bueno A., Mateu M.G., and J. M. Almendral. 2003. High mutant frequency in
36 populations of a DNA virus allows evasion from antibody therapy in an immunodeficient
37 host. J. Virol. 77: 2701-2708.
38

39
40 Lopez-Bueno, A., Valle, N., Gallego, J.M., Perez, J. and J.M. Almendral. 2004.
41 Enhanced cytoplasmic sequestration of the nuclear export receptor CRM1 by NS2
42 mutations developed in the host regulates parvovirus fitness. J. Virol. 78: 10674-10684.
43
44

45
46 Manning, G., Whyte, D. B., Martinez, R., Hunter, T., and S. Sudarsanam. 2002. The
47 protein kinase complement of the human genome. Science 298: 1912–1934.
48

49
50 Maroto, B., Ramírez, J.C., and J.M. Almendral. 2000. Phosphorylation status of the
51 parvovirus minute virus of mice particle: mapping and biological relevance of the major
52 phosphorylation sites. J. Virol. 74: 10892-10902.
53

54
55 Maroto, B., N. Valle, R. Saffrich, and J.M. Almendral. 2004. Nuclear export of the non-
56 envelopped parvovirus virion is directed by an unordered protein signal exposed on the
57 capsid surface. J. Virol. 78: 10685-10694.
58
59
60
61
62
63
64
65

1
2
3
4 Miller, C.L., and D.J. Pintel. 2002. Interaction between parvovirus NS2 protein and
5 nuclear export factor Crm1 is important for viral egress from the nucleus of murine cells.
6 *J. Virol* 76: 3257–3266.
7

8
9 Mondal, A., Potts, G.K., Dawson, A.R., Coon, J.J., and A. Mehle. 2015.
10 Phosphorylation at the homotypic interface regulates nucleoprotein oligomerization and
11 assembly of the influenza virus replication machinery. *PLoS Pathogens* 11(4):e1004826.
12
13

14 Naumer, M., Sonntag, F., Schmidt, K., Nieto, K., Panke, C., Davey, N.E., Popa-Wagner,
15 R., and J. A. Kleinschmid. 2012. Properties of the AAV assembly activating protein AAP.
16 *J. Virol.* 86: 13038-13048.
17
18

19 Parrish, C.P. 2010. Structures and functions of parvovirus capsids and the process of
20 cell infection. *Curr. Top. Microbiol. Immunol.* 343: 149-176.
21
22

23 Pillet, S., Annan, Z., Fichelson, S., and F. Morinet. 2003. Identification of a
24 nonconventional motif necessary for the nuclear import of the human parvovirus B19
25 major capsid protein (VP2). *Virology* 306, 25-32.
26
27

28 Plevka P., Hafenstein S., Li L., D'Abramo A., Cotmore S.F., Rossmann M.G., and P.
29 Tattersall. 2011. Structure of a packaging-defective mutant of minute virus of mice
30 indicates that the genome is packaged via a pore at a 5-fold axis. *J. Virol.* 85: 4822-4827.
31
32
33

34 Popa-Wagner, R., M. Porwal, M. Kann, M. Reuss, Marc Weimer, L. Florin, and J. A.
35 Kleinschmidt. 2012. Impact of VP1-specific protein sequence motifs on Adeno-
36 Associated Virus type 2 intracellular trafficking and nuclear entry. *J. Virol* 86: 9163.
37
38

39 Porwal, M., Cohen, S., Snoussi, K., Popa-Wagner, R., Anderson, F., Dugot-Senant, N.,
40 Wodrich, H., Dinsart, C., Kleinschmidt, J.A., Panté, N., and M. Kann. 2013. Parvoviruses
41 cause nuclear envelope breakdown by activating key enzymes of mitosis. *PLoS Pathog* 9:
42 e1003671.
43
44
45

46 Ramirez, J. C., Santaren, J. F., and J.M. Almendral. 1995. Transcriptional inhibition of
47 the parvovirus minute virus of mice by constitutive expression of an antisense RNA
48 targeted against the NS-1 transactivator protein. *Virology* 206: 57-68.
49
50
51

52 Ramírez, J.C., Fairén, A. and Almendral, J.M. 1996. Parvovirus Minute Virus of Mice
53 strain i multiplication and pathogenesis in the newborn mouse brain are restricted to
54 proliferative areas and to migratory cerebellar young neurons. *J. Virol.* 70, 8109-8116.
55
56
57
58
59
60
61
62
63
64
65

1
2
3
4 Reguera, J., A. Carreira, L. Riobos, J. M. Almendral, and M. G. Mateu. 2004. Role of
5 interfacial amino acid residues in assembly, stability, and conformation of a spherical
6 virus capsid. *Proc. Natl. Acad. Sci. USA*. 101: 2724-2729.
7

8
9 Riobos, L., Reguera, J., Mateu, M.G., and J.M. Almendral. 2006. Nuclear transport of
10 trimeric assembly intermediates exerts a morphogenetic control on the icosahedral
11 parvovirus capsid. *J. Mol. Biol.* 357: 1026-1038.
12

13
14 Riobos, L., Valle, N., Hernando, E., Maroto, B., Kann, M., and J.M. Almendral. 2010.
15 Viral oncolysis that targets Raf-1 signaling control of nuclear transport. *J. Virol* 84: 2090-
16 2099.
17

18
19 Ros C., N., Bayat, R., Wolfisberg, and J. M. Almendral. 2017. Cell entry of
20 protoparvoviruses. *Viruses*, 9, 313; doi:10.3390/v9110313
21

22
23 Rubio M.P., Lopez-Bueno, A., and J.M. Almendral. 2005. Virulent variants emerging in
24 mice infected with the apathogenic prototype strain of the parvovirus minute virus of mice
25 exhibit a capsid with low avidity for a primary receptor. *J. Virol.* 79: 11280–11290.
26

27
28 Sánchez-Martínez C., Grueso, E., Carroll, M., Rommelaere, J., and J. M. Almendral.
29 2012. Essential role of the unordered VP2 n-terminal domain of the parvovirus MVM
30 capsid in nuclear assembly and endosomal enlargement of the virion fivefold channel for
31 cell entry. *Virology* 432: 45-56.
32
33

34
35 Santarén, J. F., J. C. Ramírez, and J. M. Almendral. 1993. Protein species of the
36 parvovirus Minute Virus of Mice strain MVMp: involvement of phosphorylated VP-2
37 subtypes in viral morphogenesis. *J. Virol.* 67: 5126-5138.
38

39
40 Segovia, J.C., Gallego, J.M., Bueren, J.A., and Almendral, J.M. 1999. Severe
41 leukopenia and dysregulated erythropoiesis in SCID mice persistently infected with the
42 Parvovirus Minute Virus of Mice. *J Virol.*, 73, 1774-1784.
43

44
45 Sonntag, F., Bleker, S., Leuchs, B., Fischer, R., and J. A. Kleinschmidt. 2006. Adeno-
46 associated virus type 2 capsids with externalized VP1/VP2 trafficking domains are
47 generated prior to passage through the cytoplasm and are maintained until uncoating
48 occurs in the nucleus. *J. Virol.* 80: 11040-54.
49

50
51 Sonntag, F., Schmidt, K., and J. A. Kleinschmidt. 2010. A viral assembly factor
52 promotes AAV2 capsid formation in the nucleolus. *Proc. Natl. Acad. Sci. USA* 107:
53 10220-10225.
54
55
56
57
58
59
60
61
62
63
64
65

1
2
3
4 Subramaniana, S., Organtini, L.J., Grossman, A., Domeier, P.P., Cifuentes, J.O.,
5 Makhov, A.M., Conway, J.F., D'Abramo, A., Cotmore, S.F., Tattersall, P., and S.
6 Hafenstein. 2017. Cryo-EM maps reveal five-fold channel structures and their
7 modification by gatekeeper mutations in the parvovirus minute virus of mice (MVM)
8 capsid. *Virology* 510 (2017) 216–223

9
10
11
12 Sugai, A., Sato, H., Hagiwara, K., Kozuka-Hata, H., Oyama, M., Yoneda, M., and C.
13 Kai. 2014. Newly identified minor phosphorylation site threonine-279 of measles virus
14 nucleoprotein is a prerequisite for nucleocapsid formation. *J. Virol.* 88: 1140-1149.

15
16
17
18 Tattersall, P., and J. Bratton. 1983. Reciprocal productive and restrictive virus-cell
19 interaction of immunosuppressive and prototype strains of minute virus of mice. *J. Virol.*
20 46: 944-955.

21
22
23
24 Tsao, J., Chapman, M. S., Agbandje, M., Séller, W., Smith, K., Wu, H., Luo, M., Smith,
25 T. J., Rossmann, M. G., Compans, R. W. and C.R. Parrish. 1991. The three-dimensional
26 structure of canine parvovirus and its functional implications. *Science* 251: 1456-1464.

27
28
29 Tullis, G. E., Burger, L. R., and D. J. Pintel. 1992. The trypsin-sensitive RVER domain
30 in the capsid proteins of minute virus of mice is required for efficient cell binding and
31 viral infection but not for proteolytic processing in vivo. *Virology* 191: 846-57.

32
33
34
35 Tullis, G.E., R.B. Lisa, and D. J. Pintel. 1993. The minor capsid protein VP1 of the
36 autonomous parvovirus minute virus of mice is dispensable for encapsidation of progeny
37 single-stranded DNA but is required for infectivity. *J. Virol.* 67:131-141.

38
39
40
41 Ubersax, J. A., and J. E. Jr. Ferrell. 2007. Mechanisms of specificity in protein
42 phosphorylation. *Nat. Rev. Mol. Cell Biol.* 8: 530–541.

43
44
45
46
47
48
49 Valle, N., Rioloobos, R., and J. M. Almendral. 2006. Synthesis, post-translational
50 modification and trafficking of the parvovirus structural polypeptides. In *Parvoviruses*
51 (Kerr, J.R., Cotmore, S.F., Bloom, M.E., Linden R.M., and Parrish, C.R., eds), pp. 291-
52 304. Edward Arnold, London.

53
54
55
56
57
58
59
60
61
62
63
64
65 Venkatakrisnan, B., Yarbrough, J., Domsic, J., Bennett, A., Bothner, B., Kozyreva,
66 O.G., Samulski, R.J., Muzyczka, N., McKenna, R., and M. Agbandje-McKenna. 2013.
67 Structure and dynamics of adeno-associated virus serotype 1 VP1-unique n-terminal
68 domain and its role in capsid trafficking. *J. Virol.* 87:4974-4984.

1
2
3
4 Vihinen-Ranta, M., D. Wang, W. S. Weichert, and C. R. Parrish. 2002. The VP1 N-
5 terminal sequence of canine parvovirus affects nuclear transport of capsids and efficient
6 cell infection. *J. Virol.* 76: 1884-1891.
7

8
9 Wolfisberg, R., Kempf, C., and C. Ros. 2016. Late maturation steps preceding selective
10 nuclear export and egress of progeny parvovirus. *J. Virol.* 90: 5462-5474.
11

12 Xie, Q., Bu. W., Bhatia, S., Hare, J., Somasundaram, T., Azzi, A. and M.S. Chapman.
13 2002. The atomic structure of adeno-associated virus (AAV-2), a vector for human gene
14 therapy. *Proc. Nat. Acad. Sci. U S A.* 99: 10405-10410.
15
16

17
18 Yuan, W., and C.R. Parrish. 2001. Canine parvovirus capsid assembly and differences
19 in mammalian and insect cells. *Virology* 279: 546–557.
20

21 Zadori, Z., Szelei, J., Lacoste, M.C., Gariépy, S., Raymond, P., Allaire, M., Nabi, I.R.,
22 and P. Tijssen. 2001. A viral phospholipase A2 is required for parvovirus infectivity. *Dev.*
23 *Cell* 1: 291-302.
24
25

26
27 Zhang, K., Brownlie, R., Snider, M., and S. van Drunen Littel-van den Hurk. 2016.
28 Phosphorylation of bovine herpesvirus 1 VP8 plays a role in viral DNA encapsidation and
29 is essential for its cytoplasmic localization and optimal virion incorporation. *J. Virol.* 90:
30 4427-4440.
31
32
33
34
35
36
37
38
39
40
41
42
43
44
45
46
47
48
49
50
51
52
53
54
55
56
57
58
59
60
61
62
63
64
65

Legends to figures

Fig. 1. Phosphorylation status of capsid subunits in the cytoplasmic MVM assembly intermediates. **(A)** Confocal microscopy of VP subcellular distribution and nuclear capsid formation in VP-expressing NB324K cells growing asynchronously (left), synchronized at G1/S with aphidicolin (middle), and traversing S phase at 8 h post-release of the cell cycle arrest (right). Cellular DNA content determined by flow cytometry (DAPI staining) is shown to the left. CC, cell count. Scale bar, 25 μm . **(B)** Relative phosphorylation of the capsid proteins in G1/S arrested cells. Shown are ^{35}S - or ^{32}P -labeled VP proteins immunoprecipitated from supramolecular assemblies under native (n) or denaturing (d) conditions with the indicated antibodies. Gels were exposed to autoradiography for 48 h, using an intensifying screen at $-70\text{ }^{\circ}\text{C}$ for the ^{32}P -labeled samples. **(C)** Ratio of radiolabeled VP1/VP2 proteins in VP1-containing oligomers (α -VP1, native conditions) or total expressed subunits (α -VPs, denaturing conditions) quantified by densitometry of the films. Bars are means with standard errors from three independent experiments.

Fig. 2. Changes of VPs-Nt configuration during MVM assembly. IF analysis of NB324K cells transfected with the indicated pMVM-derived plasmids and maintained in asynchronous growth (*left*), or subjected to density arrest (*right*). Shown are representative confocal images of VPs subcellular distribution, and of the exposure of N-terminal domains of VP1 (1Nt) and VP2 (2Nt), as stained with specific antibodies. Bars represent average values with errors from three experiments. NA, not applicable.

Fig. 3. Nt configuration in subviral nuclear assemblies. **(A)** Cells transfected with the

1
2
3 pSVtk-VPs plasmid cultured at low density (Growing; seeding at 8×10^3 cells/cm²) or to
4
5
6 confluence (Density arrest; seeding at 8×10^4 cells/cm²) for 48h. *Left*: Flow cytometry
7
8 analysis of the percentage of transfected cells (VPs⁺) allowing capsid formation (Capsid⁺,
9
10 Mab-B7 staining). CC, cell count. *Right*: Subcellular distribution of VPs and assembly of
11
12 capsid proteins in cultures seeded at low density and confluence analyzed by confocal
13
14 microscopy. **(B)** Cells transfected with the indicated wt and single mutant VPs-expressing
15
16 plasmids cultured and analyzed as in Fig. 2. The figure shows representative confocal fields
17
18 of cells from three experiments. Average values with standard errors from three experiments
19
20 are shown.
21
22
23
24
25
26
27

28 **Fig. 4.** Exposure of the Nt domains during the MVM synchronous infection cycle. **(A)**
29 Flow-cytometry analysis of DNA content (DAPI staining), VP1-Nt exposure, and capsid
30 formation in synchronously infected NB324K cells. **(B)** Subcellular distribution, capsid
31 assembly, and access to specific antibodies recognizing the Nt domains of viral structural
32 proteins. Scale bars, 25 μ m. Shown are representative phenotypes at the indicated hours
33 post-release of isoleucine/aphidicolin arrest (hpa). Bars illustrate the average values with
34 standard errors from four experiments.
35
36
37
38
39
40
41
42
43
44
45
46
47

48 **Fig. 5.** Phosphorylation status of the protein subunits assembled in MVM particles.
49 Relative VPs phosphorylation harbored by *in vivo* ³²P-labeled empty capsid (C), and DNA-
50 filled virus (V) purified from two independent experiments. Proteins were resolved by
51 8%SDS-PAGE and either blotted to filters or fixed in the gels. *Exp.#1*: filters exposed to
52 autoradiography at -70 °C with intensifying screen (left panel), and subsequently probed
53
54
55
56
57
58
59
60
61
62
63
64
65

1
2
3
4 with the α -VPs antibody (right panel). *Exp.#2*: VPs blotted to filters (left panel) or fixed
5
6 inside the gels (right panel) prior exposure to autoradiography. Below: Ratio of VP1/VP2
7
8 signals quantified by densitometry. a.u., arbitrary units.
9

10
11
12 **Fig. 6.** VP2 phosphopeptides composition of MVM particles. *Left*: Two-dimensional
13
14 tryptic phosphopeptide maps of the VP2 subunits isolated from *in vivo* ^{32}P -labeled purified
15
16 empty and DNA-filled viral particles. TLC plates were exposed for 10 days to a radio-
17
18 analytic imaging system. Main phosphopeptides were designed as previously reported
19
20 (Maroto et al., 2000). 1D, first dimension; 2D, second dimension. *Right*: Bars represent the
21
22 signal in the films of the five major VP2 phosphopeptides quantified by densitometry from
23
24 a representative experiment. a.u., arbitrary units.
25
26
27
28
29
30
31

32
33 **Fig. 7.** Phosphorylation and Nt-configuration of capsid proteins throughout the MVM life
34
35 cycle. The diagram illustrates phosphorylation levels and exposure of Nt-domains of the
36
37 VP1, VP2 and VP3 structural proteins (respective numbers in this figure) in the supra-
38
39 molecular complexes traversing the cytoplasmic and nuclear membranes during the MVM
40
41 infection cycle. The G₁, S, and G₂ letters (connected by arrows above in the figure) refer to
42
43 the cell cycle steps at which virus assembly and maturation preferably occur. VP subunits
44
45 in the viral particles and assembly intermediates are depicted at their estimated
46
47 stoichiometry. The VP1-Nt and VP2-Nt domains are only illustrated in exposed
48
49 configuration(s) accessible to antibodies. R: Virus receptor; NPC: Nuclear pore complex.
50
51
52
53
54
55
56
57
58
59
60
61
62
63
64
65

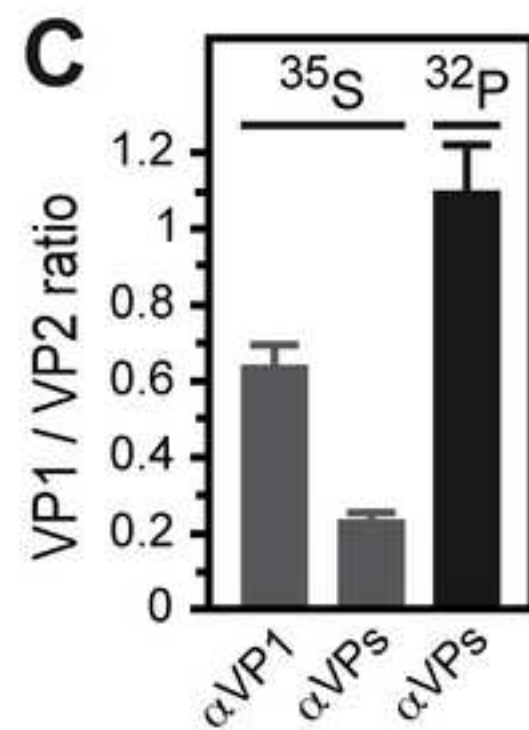
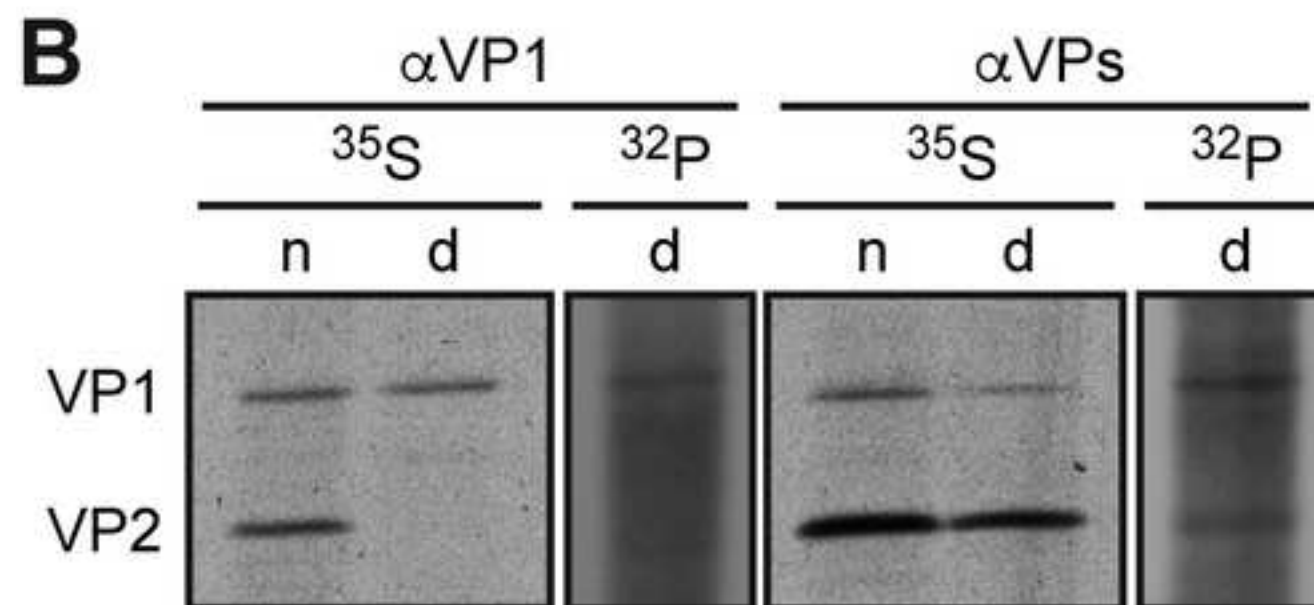
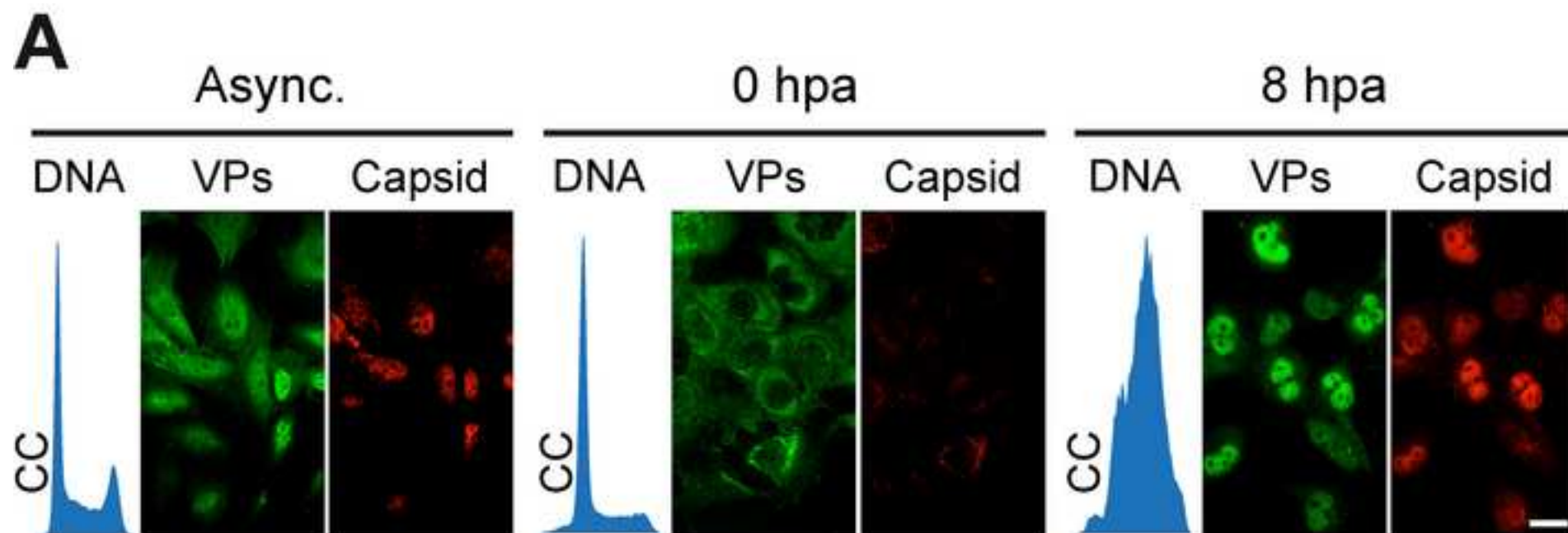


Figure 2
[Click here to download high resolution image](#)

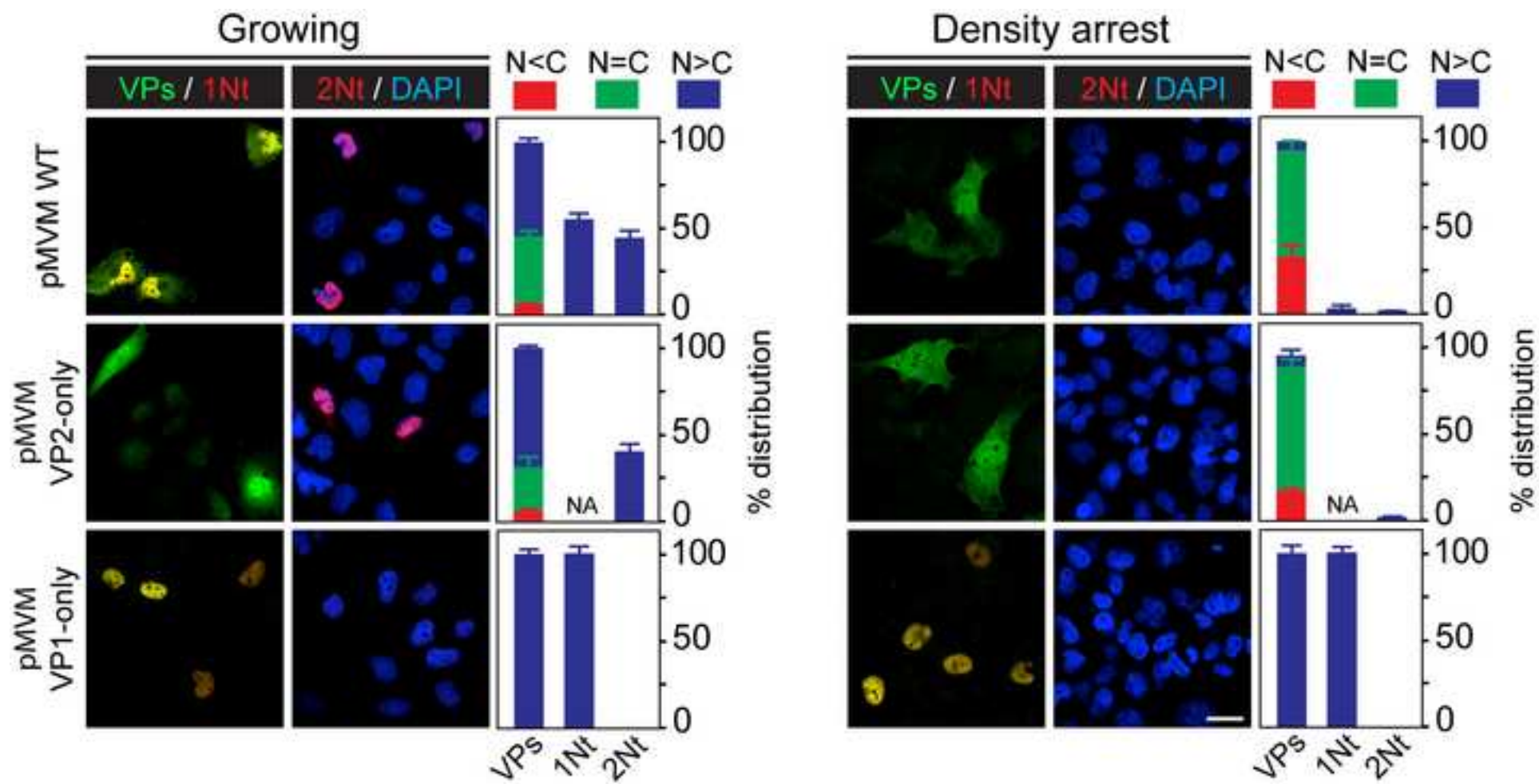


Figure 3
[Click here to download high resolution image](#)

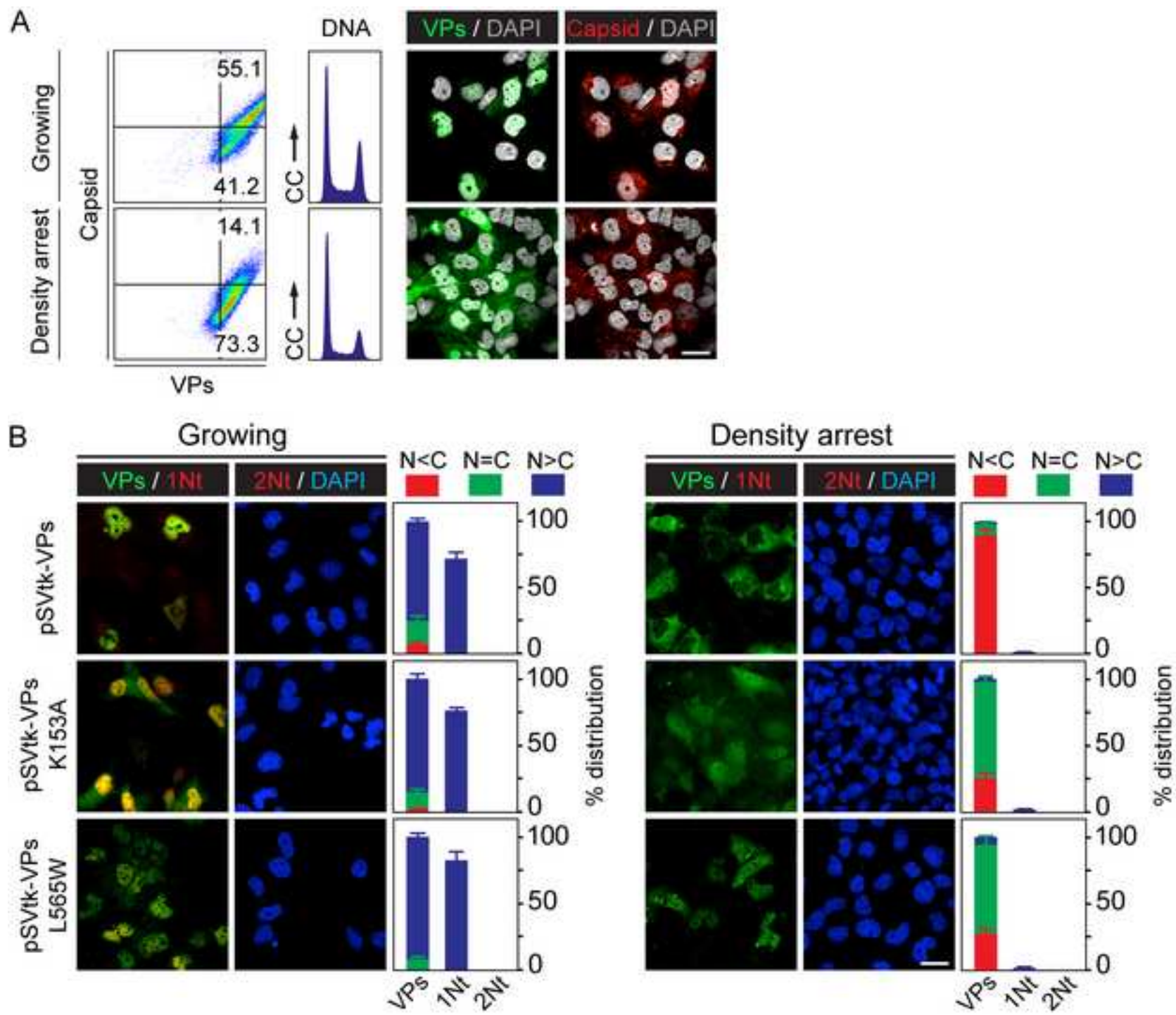


Figure 4
[Click here to download high resolution image](#)

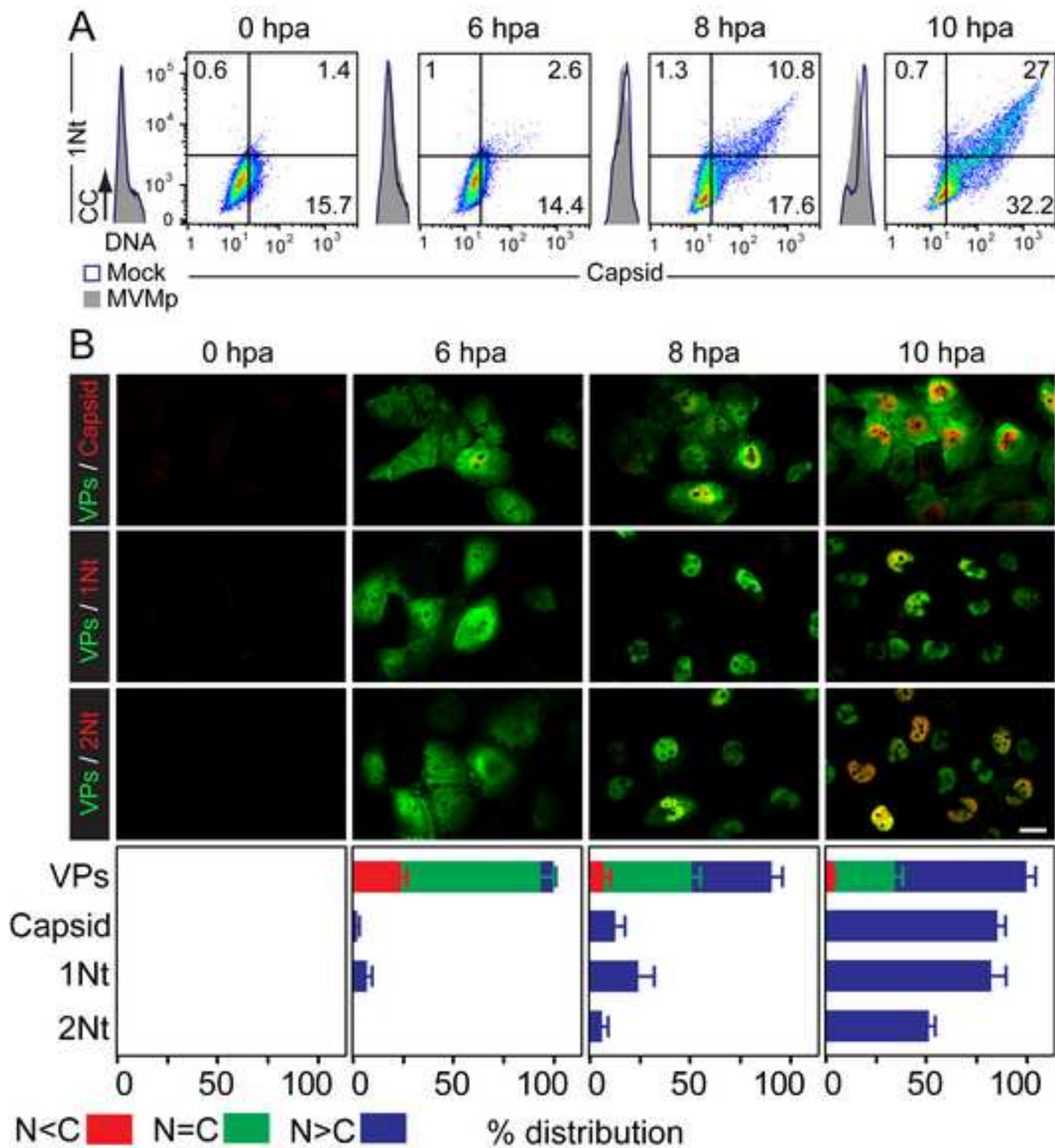


Figure 5
[Click here to download high resolution image](#)

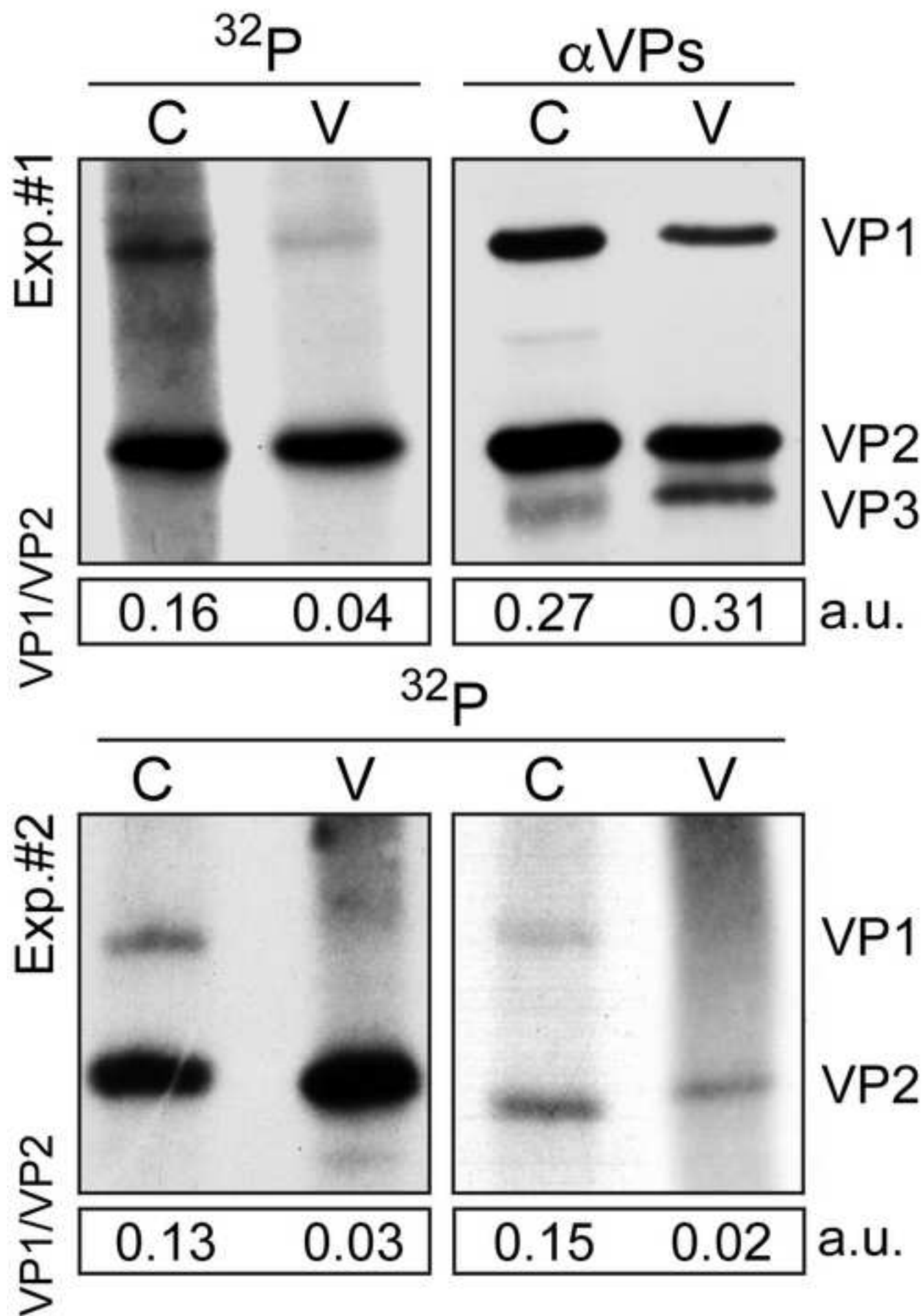


Figure 6
[Click here to download high resolution image](#)

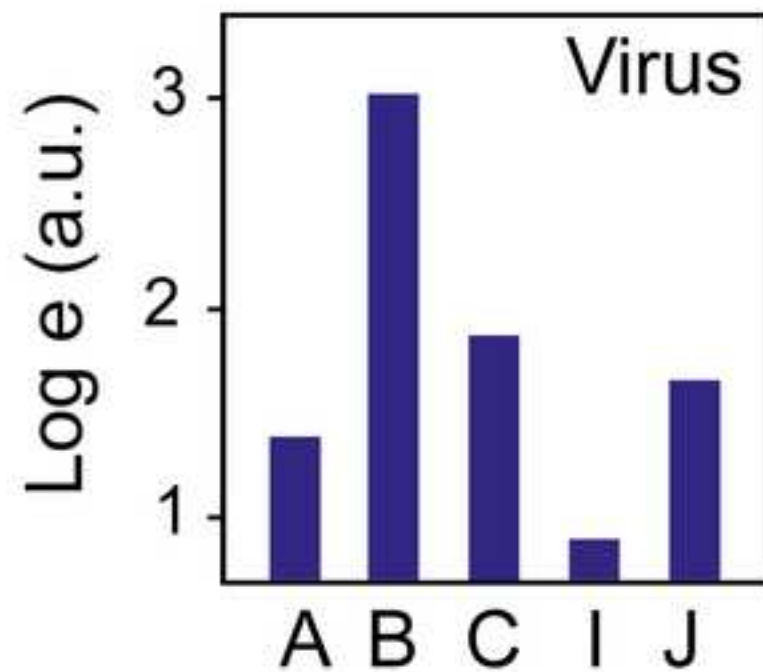
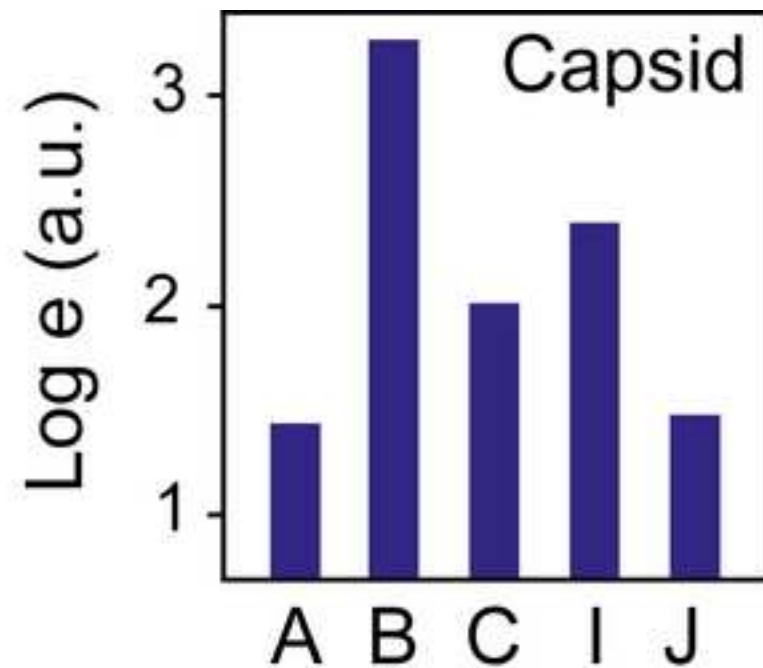
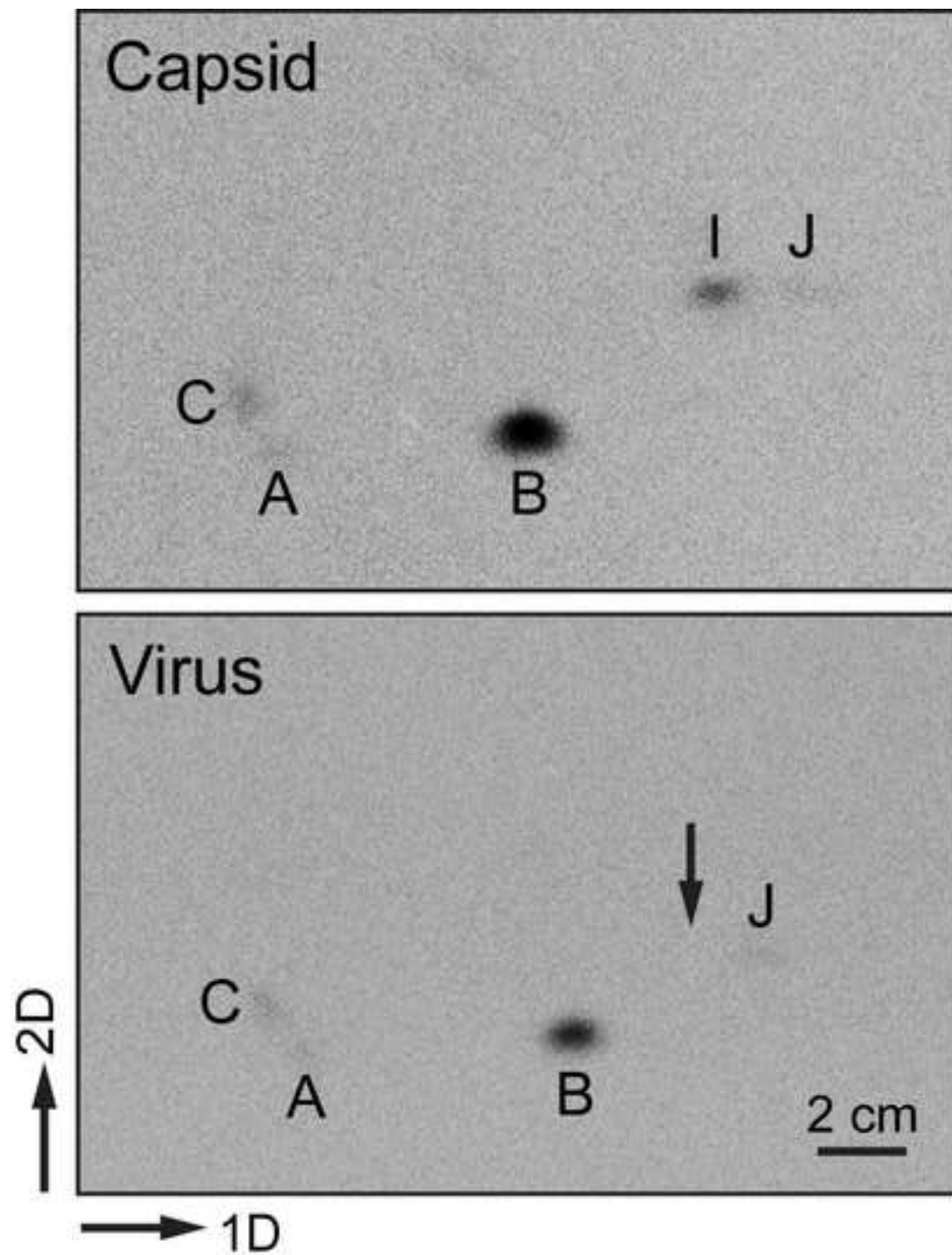


Figure 7
[Click here to download high resolution image](#)

